https://doi.org/10.5194/egusphere-2024-3905
Preprint. Discussion started: 13 February 2025

On the seasonal variability of ocean heat transport and ice shelf melt around Antarctica

Fabio Boeira Dias[1,2], Matthew H. England[1,2,*], Adele K. Morrison[3,*], and Benjamin K. Galton-Fenzi[4,5,2,*]

[1]Centre of Marine Science and Innovation, University of New South Wales, Sydney NSW, Australia
[2]Australian Centre for Excellence in Antarctic Science
[3]Research School of Earth Sciences, Australian National University, Canberra ACT, Australia
[4]Australian Antarctic Division, Hobart/Nipaluna TAS, Australia
[5]The Australian Antarctic Program Partnership, Institute for Marine and Antarctic Studies
[*]These authors contributed equally to this work.

Correspondence: Fabio Boeira Dias (f.boeira_dias@unsw.edu.au)

Abstract. The delivery of ocean heat to Antarctic ice shelves is due to intrusions of waters warmer than the local freezing point temperature. Changes in the supply of ocean heat will determine how rapidly ice shelves melt at their base, which affects Antarctic Ice Sheet mass loss and future global mean sea level rise. However, processes driving ice shelf basal melting are still poorly understood. Here we investigate the drivers of heat convergence along the Antarctic margins by performing an ocean heat budget analysis using a high-fidelity 4 km circum-Antarctic ocean–ice-shelf model. The simulation produces high basal melting in West Antarctica associated with sustained ocean heat convergence driven by advection of relatively warm deep water intrusions, with minimal seasonality in both heat supply and basal melting. For East Antarctica, ice shelves have substantial basal melt seasonality, driven by strong air-sea winter cooling over the continental shelf depressing shallow melting, while in summer, increased heat inflow towards the ice shelves is driven by surface-warmed waters that subduct under shallow regions of ice, increasing melt. The high seasonality of basal melting in East Antarctic ice shelves is responsive to interactions between the atmospheric forcing, the local icescape, and the activity of polynyas. Our results suggest that seasonal changes in future climate change scenarios are critical in determining the duration and intensity of air-sea fluxes with substantial impacts on ice shelf basal melting and ice sheet and sea level budgets.

1 Introduction

Ocean heat delivery towards Antarctica is a key driver of ice shelf basal melting, where changes in heat transport can drive ice shelf thinning and grounding line retreat, with implications for ice sheet stability and future global sea-level changes. The stability of the Antarctic Ice Sheet, which holds the equivalent of 58 m of global mean sea-level rise (Fretwell et al., 2013), depends on the buttressing effect from floating ice shelves that impede ice flow towards the ocean (Joughin et al., 2010). Satellite observations show that the Antarctic ice sheet lost mass over the last few decades (Adusumilli et al., 2020), of which about half is due to ocean-driven basal melting of the ice shelves (Rignot et al., 2013; Pritchard et al., 2012), highlighting the importance

https://doi.org/10.5194/egusphere-2024-3905
Preprint. Discussion started: 13 February 2025

of the Antarctic coastal ocean circulation and dynamics for sea-level projections.

The latest sea-level projections relied on climate models outputs to force ice sheet models under ISMIP6 (Edwards et al., 2021; Seroussi et al., 2024). However, the ocean component of CMIP5 and CMIP6 models have often coarse (1°) horizontal resolution (∼55 km at 60°S), inherent biases in continental shelf temperatures (Purich and England, 2021), and lack active ice-shelf and ice-sheet coupling (Fox-Kemper et al., 2023). At 1° horizontal resolution, eddies, tides and other small-scale processes at the continental shelf (Stewart et al., 2018; Jourdain et al., 2019; Hausmann et al., 2020), such as Antarctic Bottom Water formation (Heuzé, 2021) and channelised flow associated with bathymetric troughs (Drews, 2015; Alley et al., 2016; Marsh et al., 2016; Milillo et al., 2019) are not resolved. The lack of ocean–ice-shelf-ice sheet coupling means that feedbacks between the ocean-atmosphere-cryosphere system are also not properly resolved; neither some essential features of the icescape, such as landfast sea ice (Fraser et al., 2023), icebergs (Merino et al., 2016) and the ice shelf front. The Antarctic Ice Sheet contribution to CMIP6 sea-level projection has the largest uncertainty among all contributors to global mean sea-level changes (Fox-Kemper et al., 2023). A leading source of the uncertainty is due to the differences between ice sheet models (Seroussi et al., 2023), with limitations in the ocean forcing being critical.

Ocean heat delivery to the ocean–ice-shelf boundary layer (i.e., available for basal melting) is determined by the vertical mixing and thermohaline circulation in the sub-ice shelf cavities (Rosevear et al., 2024). Jacobs et al. (1992) described three modes of basal melting associated with ocean temperature and density. Mode 1 melting is induced by the inflow of high-salinity Dense Shelf Water (DSW), formed at winter coastal polynyas, flowing towards the grounding line. Despite being cold, DSW is above the local freezing point temperatures at depths close to the grounding line. This mode of melting is usually observed within cold ice shelf cavities such as the Filchner-Ronne, Ross and Amery ice shelves (Thompson et al., 2018). Mode 2 melting is driven by the inflow of Circumpolar Deep Water (CDW) at intermediate-depths of the cavities, which is associated with ice shelves within a warm regime, such as those in the West Antarctic sector (Thompson et al., 2018). Mode 2 is associated with high melt rates since CDW can be up to 3°C above the local freezing point temperature at the deep parts of the cavity (Jenkins et al., 2010); examples are Pine Island and Thwaites in the Amundsen-Bellingshausen sector and the Mertz and Totten in East Antarctica (Silvano et al., 2016). Mode 3 melting is associated with shallow melting near the ice shelf calving front, driven by seasonally warmed waters along the coastal currents; this mode has been observed in the ice front of the Filchner-Ronne, Fimbul and Ross ice shelves (Makinson and Nicholls, 1999; Joughin and Padman, 2003; Arzeno et al., 2014; Stewart et al., 2019).

Despite substantial progress in understanding basal melting through in situ observations, these measurements are extremely difficult to obtain and are sparse in both locations and time. Given the harsh conditions, it requires either drilling through hundreds of metres of ice or using autonomous platforms and floats (Miles et al., 2016; Friedrichs et al., 2022; Sallée et al., 2024). Satellite-derived maps of Antarctic basal melting show high spatial variability of the melt rates (Rignot et al., 2013; Adusumilli et al., 2020), especially between cold and warm ice shelves. Cold-water ice shelves are thought to be dominated by

https://doi.org/10.5194/egusphere-2024-3905
Preprint. Discussion started: 13 February 2025

mode 1 melting (i.e., DSW-driven) near the grounding zone (e.g., Ronne Ice Shelf) and mode 3 (i.e., driven by warm surface waters) in the shallow portion of the ice draft; warm-water ice shelves are dominated by mode 2 melting (i.e., CDW-driven). However, the temporal variability of these satellite datasets has not been validated yet (Vaňková and Nicholls, 2022). Observational efforts, such as those using the ApRES (autonomous phase-sensitive radar) system (Nicholls et al., 2015) brought substantial understanding of the intra-annual variability in some ice shelves (Cook et al., 2023; Lindbäck et al., 2019; Davis et al., 2018; Sun et al., 2019), while highlighting disagreement between satellite and in situ melt rates (Vaňková et al., 2021; Lindbäck et al., 2023). Given these limitations, here we take advantage of a high-resolution ocean-ice shelf model to describe the circum-Antarctic basal melting variability at intra-annual scale.

Given the importance of basal melt as a key parameter for Antarctic Ice Sheet stability and its future contribution to global sea level, progress towards a better understanding of the main mechanisms driving heat transport into the ice shelf cavities, the relative importance of different basal melting modes, and physical drivers of the temporal variability of basal melting are urgently needed. This study examines these aspects using a realistic simulation from the Whole Antarctic Ocean Model (WAOM, Richter et al., 2022a), a high-fidelity circum-Antarctica ocean–ice-shelf model of high (4 km) horizontal resolution including tides (Richter et al., 2022b). More details on WAOM and the ocean heat budget analyses used for process-based investigation are presented in Section 2. The annual and seasonal links between ocean warming within the ice shelf cavities and basal melting, and the physical drivers, are presented in Section 3.1. The temporal variability of heat transport processes across different regions is presented in Section 3.2 and their driving mechanisms are explored in Section 3.3, followed by discussion and conclusions in Section 4.

2 Methods

The analyses presented here were performed using a simulation from the WAOM setup of the Regional Ocean Modeling System (ROMS Shchepetkin and McWilliams, 2005), which has a grid with a south polar projection of uniform horizontal resolution. WAOM includes thermodynamic interactions via three-equation parameterisation (Galton-Fenzi et al., 2012; Holland and Jenkins, 1999) with static ice shelves from Bedmap2 (Dinniman et al., 2007; Fretwell et al., 2013). Here we use WAOM at 4 km, as the mechanisms described here hold both for coarser (10 km) and finer (2 km) resolutions which is an intermediate commitment in terms of storage (especially regarding the daily heat budget diagnostics, see below). The WAOM simulation was run for 10 years and started from the 10 km WAOM simulation at year 10 (10 km initialised from WOA13 hydrography). WAOM is forced with a repeat year forcing approach using 2007 as a representative year of the present-day state Richter et al. (2022a).

The ocean surface is forced with prescribed surface heat and salt fluxes associated with sea ice growth and melting derived from sea-ice estimates from satellites (Tamura et al., 2011) — representing important aspects of the ocean-sea ice interaction

https://doi.org/10.5194/egusphere-2024-3905
Preprint. Discussion started: 13 February 2025

such as the spatial extent of realistic coastal polynyas, and sites of DSW formation, that are not recoverable using existing sea ice models (Dias et al., 2023). Tidal forcing is included using both velocities and surface elevation at the northern boundaries using 13 major constituents from TPXO7.2 (Egbert and Erofeeva, 2002). Lateral conditions are imposed with daily reanalysis from ECCO2 (Dee et al., 2011), daily surface winds at 10 m are obtained from ERA-Interim — combined with monthly relaxation to SOSE sea surface temperature (Mazloff et al., 2010). Previous comparison has shown WAOM produces cold bottom temperature biases in the Bellingshausen Sea and, to a lesser extent, in the Amundsen Sea (thus underestimating basal melting in this sector) and fresher biases in the Weddell Sea (Dias et al., 2023), possibly associated with the surface buoyancy forcing from Tamura et al. (2008). Low formation of DSW in the first version of WAOM (Richter et al., 2022a) has been improved in Dias et al. (2023) by fully accounting for the surface salt flux estimates from satellites, which were limited due to a mismatch between forcing and simulated surface fields. More details on the WAOM configuration and evaluation can be found in Richter et al. (2022a, b) and (Dias et al., 2023).

2.1 Ocean Heat Budget analyses

The ocean heat budget analyses were performed for the entire circumpolar Antarctic continental shelf (including the sub-ice shelf cavities) for ease of analysis were divided into bins of 3° longitude (latitudinal-bins in the east side of the Antarctica Peninsula due to the shape of Antarctica, Figure 1a). We saved daily outputs of heat flux convergences (°C s^{-1}) for all the temperature equation terms:

$$\frac{\partial}{\partial t}\left(c_p\ \rho\ \theta\right) = -\nabla \cdot \left[c_p\ \rho\ \left(v\theta + F\right)\right] + Q_{sfc} \tag{1}$$

where c_p is the specific heat capacity of seawater (3989.25 J kg^{-1} $°C^{-1}$), ρ is the potential density (kg m^{-3}), θ is the potential temperature in degrees Celsius, and v is the speed of the ocean, F represents subgridscale processes, and Q_{sfc} is the net surface heat flux. On the right-hand side, the product $v\theta$ represents the heat convergence due to the resolved model advection (hereafter referred to as ADV), while F represents the subgridscale processes ($DIFF$) not resolved by the model's advection scheme. $DIFF$ is only due to Laplacian horizontal mixing with a coefficient of 20 $m^2 s^{-1}$ that has a diffusive effect on heat in the down-gradient direction. Vertical mixing associated with the K-profile parameterisation used in the model (KPP; Large et al., 1994) is equal to the surface fluxes when vertically integrated — linked with the buoyancy (Tamura et al., 2011) and mechanical (Dee et al., 2011) forcing (outside the ice shelf cavities) — these are all included in the surface flux term Q_{sfc} (hereafter called SFC). The left-hand side represents the net heat tendency (NET) and is exactly equal to the sum of all the processes on the right-hand side. All the analyses presented here use daily mean diagnostics outputs from the last simulated year of the 4 km WAOM simulation (year 10, Figure A2).

https://doi.org/10.5194/egusphere-2024-3905
Preprint. Discussion started: 13 February 2025

3 Results

3.1 Physical drivers of basal melting of the Antarctic ice shelves

The ocean-driven melting of the Antarctic ice shelves has a direct relationship with the heat available — as described by the different modes of melting discussed in Jacobs et al. (1992). Maps of annual ocean heat transport (depth-integrated) and basal melt rates are shown in Figure 1a. Ice shelf basal melting integrated horizontally for each 3° bin is shown in Figure 1a. Basal melt rates higher than ∼10 Gt/yr are widespread around the Antarctic continent and are located on well-known ice shelves, such as: Getz, Pine Island, Thwaites, Larsen C, and Filchner-Ronne ice shelves in West Antarctica; and Fimbul, Amery, Shackleton, Totten, Mertz, and Ross ice shelves in East Antarctica. To identify the seasonal variability in the basal melting, summer (red; defined as December to May) and winter (blue; June to November) averages of the basal melting are shown compared with the annual mean (black). A clear seasonal cycle is found in some but not all ice shelves — in particular there is high seasonality along the East Antarctic sector. Whereas the majority of melting in the West Antarctic sector exhibits relatively stable melt rates throughout the year. Based on the melting variability between summer and winter averages compared with the annual average, we classify the Antarctic ice shelves into either a seasonal melt regime or a steady melt regime, shown in green/orange colors in Figure 1a: seasonal melting is defined when the seasonal melt rates (either winter or summer averages) are larger than the annual mean ± 20%; otherwise, it is defined as steady melting. Although we classify the Filchner-Ronne Ice Shelf (FRIS) into the steady regime, this is due to our framework requirement of averaging across the 3° longitude ice shelf cavity bins at FRIS, which leads to cancellation between different phases of melting inside the cavity due to the distinct pathways along which warm anomalies are transported within the cavity (Dias et al., 2023; Vaňková and Nicholls, 2022). Observations show that FRIS exhibits two seasonal maxima in the melting variability (Fig. 7 in Vaňková and Nicholls, 2022).

To understand the drivers of the seasonal melting, the depth-integrated total heat transport convergence (ADV plus $DIFF$ in Eqn. 1) was also integrated horizontally for each bin, first only within the ice shelf cavities (Figure 1c), but also over the whole continental shelf (including the ice shelf cavities, Figure 1d). The heat transport term integrated meridionally over the continental shelf describes the effect from the cross-slope heat transport plus the zonal convergence at each longitude bin, while the integral over the ice shelf cavities represents the transport across the ice shelf front plus zonal convergence within the ice shelf cavity. This means that the heat transport convergence includes the effect from water masses traveling zonally along the continental shelf before entering the ice shelf cavity, while these water masses are also subjected to air-sea fluxes within the continental shelf.

This impact of the air-sea fluxes on the heat convergence is substantial, given the differences in magnitude of the heat transport convergence in the continental shelf and within the ice shelf cavities (Figure 1c,d). The correlation between the annual mean heat convergence integrated meridionally over the continental shelf and within the ice shelf cavities is indeed low (r^2 = 0.12). Besides the low correlation, the seasonality also differs between the continental shelf and ice shelf cavities, where the latter has a clear seasonality in the heat convergence within some ice shelves (e.g., East Antarctica, Figure 1c) but not in all of

https://doi.org/10.5194/egusphere-2024-3905
Preprint. Discussion started: 13 February 2025

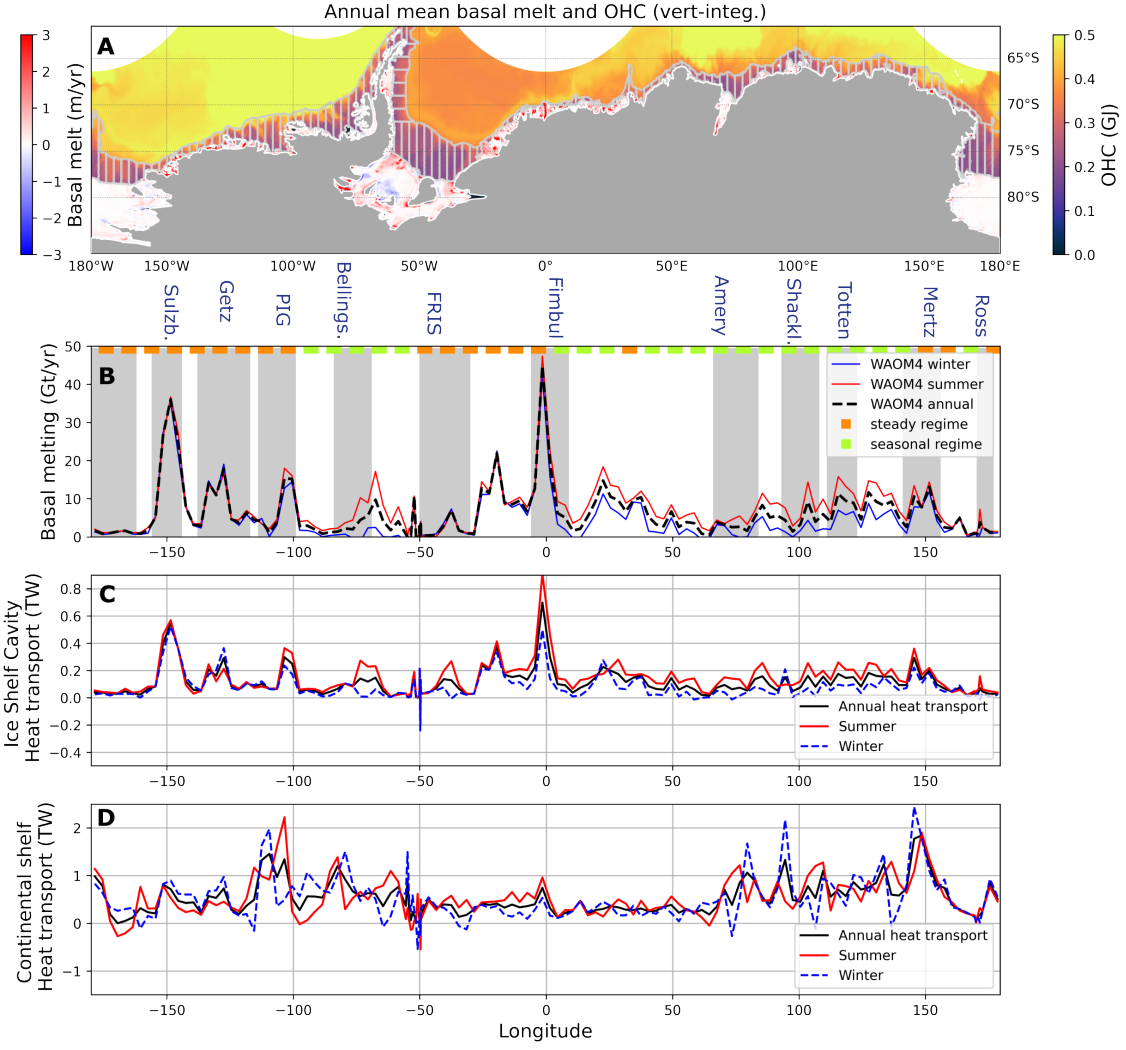

Figure 1. (a) Maps of annual averaged (over the last simulated year) ocean heat content vertically-integrated (GJ = 1x10^9J, shown everywhere except at the ice shelf cavities), and annual averaged basal melt rates (m/yr). (b) shows the basal melt rates integrated over each longitudinal bin (Gt/yr, 1 Gt = 1x10^{12} kg), shown as annual (black dashed line), summer (December-May, red line) and winter (June-November, blue line) averages. The ocean heat transport ($ADV + DIFF$) horizontally- and vertically-integrated for each longitudinal bin (TW, 1 TW = 10^{15}W) is shown in (c) only for the ice shelf cavities and (d) for the whole continental shelf — also shown as annual (black), winter (red) and summer (blue) averages. Subregions selected for the timeseries analyses presented in Figures 3, A4, A5, and A6 are shown in shaded gray in (b). The ice shelf melt regimes were classified into seasonal regime (green in panel b; when summer or winter melt rates are equal or larger than the annual mean ±20% but re-binned into 9° longitude intervals), or steady regime (orange, for the remaining cases).

https://doi.org/10.5194/egusphere-2024-3905
Preprint. Discussion started: 13 February 2025

them, while the heat convergence over the continental shelf does not exhibit a clear seasonality.

High basal melt and heat transport into the ice shelf cavities (Figure 1b,c), however, are closely related with a time-mean spatial correlation r^2 of 0.90. Moreover, the seasonality in the heat transport aligns with melt regime classification: strong heat transport seasonality into ice shelves is colocated with seasonal melting (e.g., East Antarctica) and insignificant heat transport seasonality occurs for non-seasonal melt ice shelves in the Amundsen Sea. This indicates that heat transport (mostly controlled by ADV, see Figure 2) primarily controls the seasonality in the basal melt. The only exception is the Filchner-Ronne Ice Shelf as previously described, which shows seasonality in the heat transport but not in the basal melting (Figure A5).

We now look at the full ocean heat budget to understand the relationship between distinct heat transport processes. Individual processes, i.e., advection, horizontal diffusion and surface fluxes, contribute to the net heat tendency (left-hand side in Eqn. 1). The annual mean ocean heat budget results from a balance between winter and summer contributions. We discuss the seasonal ocean heat budget integrated meridionally only within the ice shelf cavities (Figure 2a) and over the continental shelf (Figure 2b), while the annual budget is shown in the Supplemental Material (Figure A1). Both over the continental shelf and within the ice shelf cavities, the net heat tendency (NET) is the residual between opposite contributions from the total heat transport (ADV+$DIFF$) and the surface fluxes (SHF). Horizontal advection (ADV, yellow line) and horizontal diffusion ($DIFF$, green line) converge heat (total heat transport in Figure 1c,d) and counter-balance the cooling from the net surface heat flux (SHF, blue line). Over the continental shelf, the SHF is the main driver of the seasonal cycle (blue lines in Figure 2b), associated with strong atmospheric cooling during winter, when the continental shelf temperature decreases and sea ice is formed. Strong cooling is associated with coastal polynyas, where persistent katabatic winds maintain an ice-free region adjacent to the coast (or ice front or fast-ice), sustaining high sea-ice production and offshore export (Ohshima et al., 2016). Regions with fewer coastal polynyas, such as around the Dronning Maud Land region (around 0° longitude), present much milder wintertime cooling than some sectors in the East (70-150°E) and West (60-110°W) Antarctic (dashed blue line in Figure 2b; Tamura et al. 2011).

The seasonality in the horizontal advection and diffusion over the continental shelf (Figure 2b) are less evident than in the surface fluxes. $DIFF$ represents parameterised lateral diffusive heat fluxes acting down-gradient at strong frontal regions such as the Antarctic Slope Front, with a negligible seasonal cycle in the Antarctic margins. ADV is associated with the ocean circulation, accounting for both cross-shelf (or cross-calving front) heat transport and the zonal heat convergence associated with the slope and coastal currents. The advection term has substantial seasonal variability, although the direction of seasonal change varies spatially.

Within the ice shelf cavities (Figure 2a), the seasonal variability has different drivers compared to those operating on the continental shelf. In the ice shelf cavities, both advective (ADV) and diffusive ($DIFF$) heat transport balance the heat extracted from the ocean to melt ice (SFC) — which is larger where the heat transport is also large (Figure 1c,d). The seasonal variabil-

https://doi.org/10.5194/egusphere-2024-3905
Preprint. Discussion started: 13 February 2025

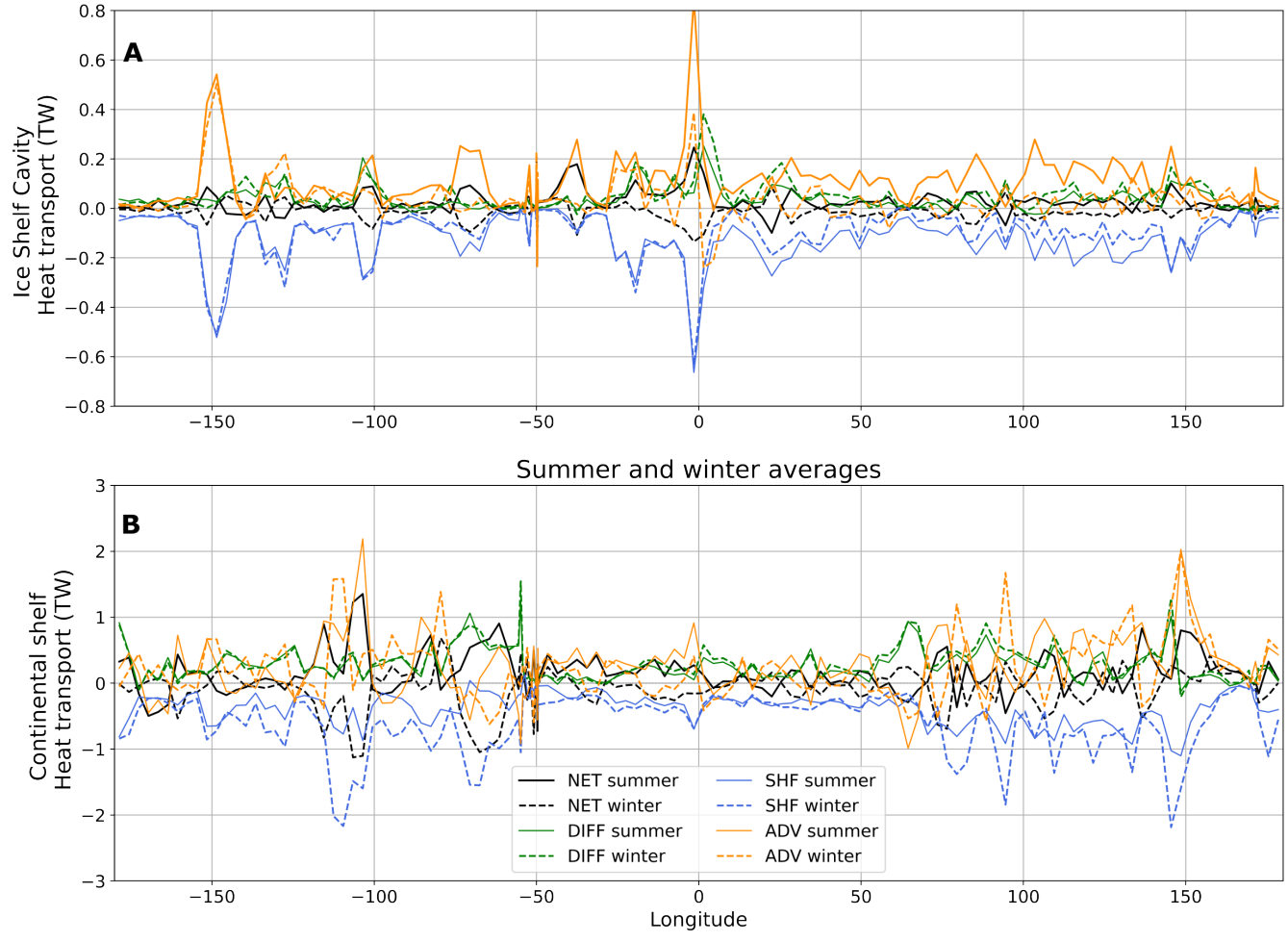

Figure 2. Ocean heat budget horizontally- and vertically-integrated over longitudinal bins (in TW) for the whole continental shelf (including ice shelf cavities, upper panel) and only the ice shelf cavities (lower panel). Processes are shown in green ($DIFF$), blue (SHF), yellow (ADV) and black (NET). Summer (average December to May of the last simulated year, solid line) and winter (average June to November, dashed line) are shown. Positive (negative) heat flux convergences denotes warming (cooling).

ity of the total heat transport is driven mostly by advection, with only a secondary contribution to the seasonality from diffusion.

Seasonality of the heat transport (ADV+$DIFF$) and SFC are only large at those ice shelves with a seasonal melt regime (mostly in the East Antarctic, between 0-150°E, Figure 1d), presenting a maximum in summer and minimum in winter. In contrast, for the steady melt regime in the West Antarctic ice shelves (centred at 150°W, 130°W, 105°W), heat transport and SFC have substantially less seasonality. The results from the ocean heat budget indicate that the temporal variability in the

https://doi.org/10.5194/egusphere-2024-3905
Preprint. Discussion started: 13 February 2025

advection term (with a secondary contribution from diffusion) is key for basal melt variability.

3.2 Sub-seasonal variability of basal melting

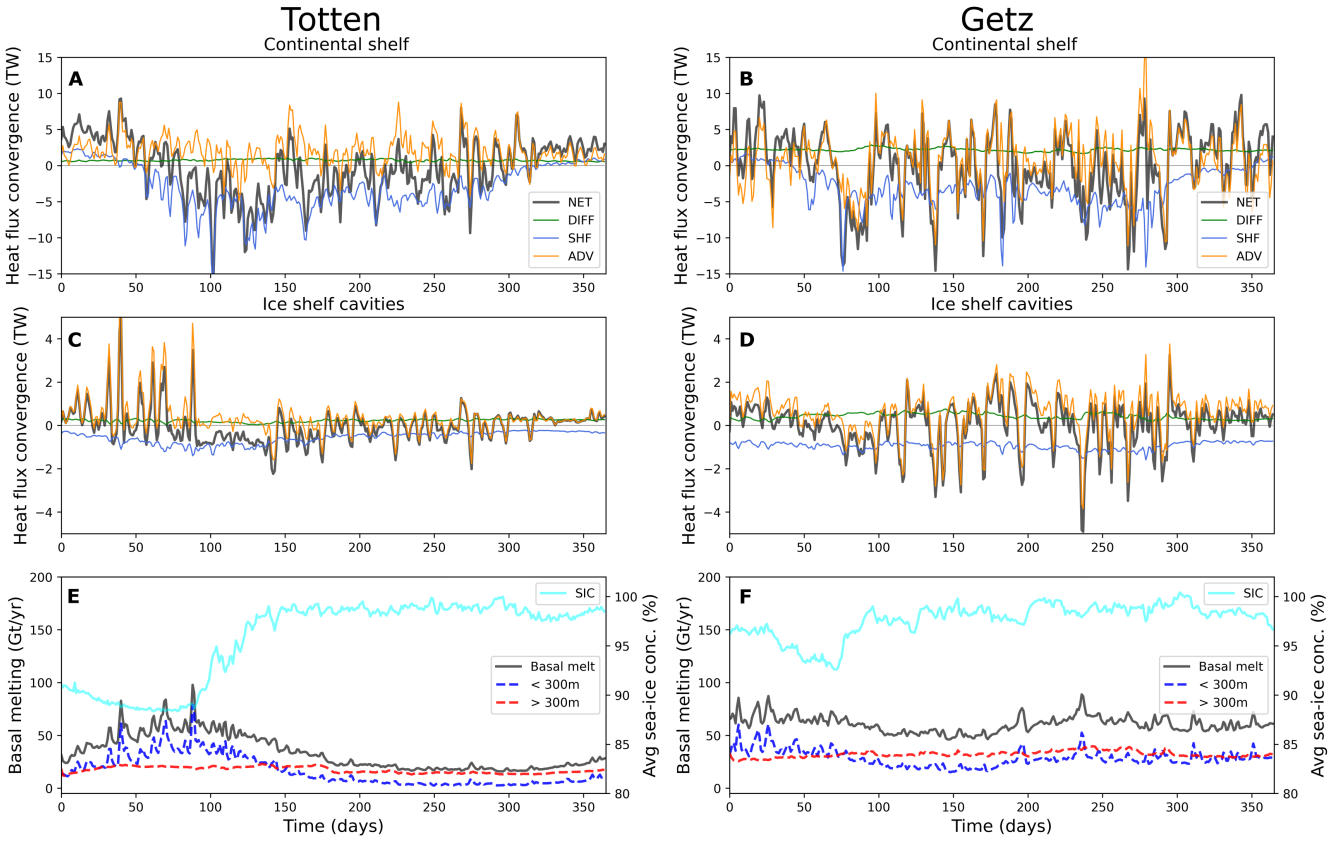

Figure 3. Daily averaged (over the last simulated year) ocean heat budget horizontally- and vertically-integrated over the vicinity of the Totten Ice Shelf (left column) and the Getz Ice Shelf (right column); shown as examples of seasonal and steady melt regions, respectively. (a) and (b) show the heat budget for the whole continental shelf, (c) and (d) show the heat budget for the ice shelf cavities. Net heat tendency (NET) is shown in black lines and processes are shown in blue (SFC), green ($DIFF$), and orange (ADV); positive (negative) heat convergence translates to a warming (cooling) effect within the integrated region. (e) and (f) show the basal melt rates (black, horizontally-integrated), sea-ice concentration (cyan, averaged).

To analyse the drivers of sub-seasonal variability of basal melting around Antarctica, we integrate the ocean heat budget terms over eleven selected subregions, based on high basal melt rates (gray shadings in Figure 1b), which were classified into 1) seasonal melt or 2) steady melt regimes. We closely investigate the Totten Ice Shelf (as an example of the seasonal regime)

https://doi.org/10.5194/egusphere-2024-3905
Preprint. Discussion started: 13 February 2025

and the Getz Ice Shelf (as an example of the steady regime) in this and the next section. Other high melting regions are presented in the Supplementary Material for completeness.

The daily heat budget for the Totten (1) and Getz (2) ice shelf regions are shown in Figure 3. Most processes described here for these two examples generally hold for other subregions classified within the respective regimes, with the exception of Filchner-Ronne Ice Shelf as mentioned previously. The melting regime in the Totten Ice Shelf (Figure 3, left column), has an elevated basal melt rate of up to 100 Gt/yr between late January and May (from day 1 to around day 150, Figure 3e, black line). This melt is a response to heat convergence ($>$ 2 TW) driven by the ocean circulation (ADV, Figure 3c). The high temporal variability of the advection component (timescale of a few days) suggests that transient processes such as mesoscale eddies, storm-driven effects on coastal circulation, and/or coastal waves could be the driver of these warming events. Basal melt starts to decline in April ($\sim$ day 100), which coincides with the abrupt reduction in the ADV warming and rapid SFC cooling over the continental shelf (Figure 3a,c,e). Melt reaches a minimum ($<$ 15 Gt/yr) in August-October (days 230-310). The surface heat loss is associated with the rapid increase in sea-ice concentration (measured from satellites and accounted for in WAOM via surface buoyancy forcing) as a result of the wintertime expansion (cyan line in Figure 3e).

In the Getz Ice Shelf (Figure 3b,d), the steady melt regime is associated with advective heat convergence during most of the year. Large positive ADV is found (2 TW) — similar to the Totten region during summer — and the basal melt rate maintains a minimum of around 50 Gt/yr (Figure 3f). The ADV warming effect also occurs through transient episodes. The sea-ice concentration (cyan line in Figure 3f) has a smaller seasonal variation in the Getz region than in the Totten, suggesting sea-ice related processes could be important to differentiate the two regimes. WAOM does not include an active sea-ice component, although it represents some of its effects through the prescribed surface buoyancy fluxes from Tamura et al. (2008). Effects from the wind fields are also taken into account in the surface buoyancy forcing, such as for the impact of katabatic winds on coastal polynyas. An interpretation of the underlying mechanisms is explored below.

3.3 Mechanisms of seasonal heat advection into Antarctic ice shelf cavities

To describe the mechanisms sustaining the different regimes of basal melting, we examine bottom temperature (mean and seasonal anomalies) and the surface heat flux (Figures 4 and 5). In the Totten, seasonal bottom temperature anomalies suggest a link with the surface heat fluxes (Figure 4e,f). Wintertime cooling from the Dalton Polynya, the main coastal polynya in the Totten basin, spreads along the ocean floor towards the ice shelf front from June to November (winter anomaly is shown in Figure 4e,f). Monthly anomalies show that local cold anomalies move westward in several regions of the East Antarctic sector (Mertz, Totten, Shackleton, Amery, and Fimbul ice shelves; not shown), likely associated with the Antarctic Coastal Current. This feature indicates the advection of ocean heat in regions downstream of large coastal polynyas can influence basal melting nearby.

https://doi.org/10.5194/egusphere-2024-3905
Preprint. Discussion started: 13 February 2025

In summer months, the ocean near the Totten ice shelf front region warms, causing enhanced shallow (< 300 m) melting. This warming is also seen to propagate westward with the Antarctic Coastal Current. Waters in the upper-300 m have large seasonal variability (Figure 4d,g), alternating between fresh Antarctic Surface Waters in February to Winter Waters in August, with near surface freezing point temperature and relatively high salinity waters. Below 300 m, less variability is seen in the ocean properties, indicating that modified Circumpolar Deep Water (mCDW) drives deep melting within the Totten Ice Shelf.

The mechanisms observed in the Totten region are also observed near other ice shelves in the East Antarctic with seasonal melt regimes, such as Fimbul, Amery (Figures A5, A11, A12), Shackleton, Mertz and Ross ice shelves (Figures A6 and A13, A14 and A15). The Bellingshausen Sea presents a seasonal melt regime in this simulation at 4 km (Figure A4 and A9), although this region is cold-biased in relation to the observations (Schmidtko et al., 2014) and so potentially underestimates the basal melt. WAOM at 10 km shows more CDW intrusion and higher basal melt rates (Dias et al., 2023), in better agreement with observations (not shown).

In the vicinity of the Getz Ice Shelf (Figure 5), different mechanisms dominate the melting variability. Bottom temperature anomalies show some seasonality, but their actual impact on the melt rates is almost negligible. The surface heat flux at the Amundsen Sea Polynya (Stammerjohn et al., 2015) is nearly as strong as the Dalton Polynya, but there is less evidence of deep convection from the bottom temperature anomalies in winter (Figure 5e,f), due to a stronger vertical stratification of the ocean. Winter bottom temperature anomalies are concentrated along the shelf break and the Dotson trough, showing considerable warming. In summer, mild bottom cold anomalies are found within the region. Importantly, these winter and summer anomalies are away from the ice shelf front, and therefore have little impact on the seasonal shallow melting, as seen for the Totten Ice Shelf. Basal melt maps for both seasons are fairly similar in most regions on the Getz cavity, and in particular for the deep parts of the cavity. Seasonal formation of Antarctic Surface Waters and Winter Waters dominate the upper-200 m, while at depths below 400 m the supply of mCDW is relatively constant through the year (Figure 5d,g). A similar process also dominates other steady regime regions, all located in the Amundsen Sea: the Sulzberger Ice Shelf and the Dotson-Thwaites-Pine Island region (heat budget time series for these regions are shown in Figures A4, A7, A8 and A9).

4 Discussion and conclusions

In summary, this study employed a circum-Antartic ocean–ice-shelf model under a prescribed atmosphere-sea ice repeat year forcing for 2007 in order to investigate the drivers of intra-annual variability of basal melting. Our results show that most Antarctic ice shelves exhibit either a seasonal or steady melt regime over these timescales. The variability of the basal melt is directly driven by the total ocean heat transport within the ice shelf cavities (Figure 1b,c). The melting of ice shelves in East Antarctica is predominantly seasonal, driven by a striking contrast between ice front cooling in winter forced by coastal polynya activity, and summertime warming of waters that penetrate into the upper-300 m portion of the ice shelf cavities driv-

https://doi.org/10.5194/egusphere-2024-3905
Preprint. Discussion started: 13 February 2025

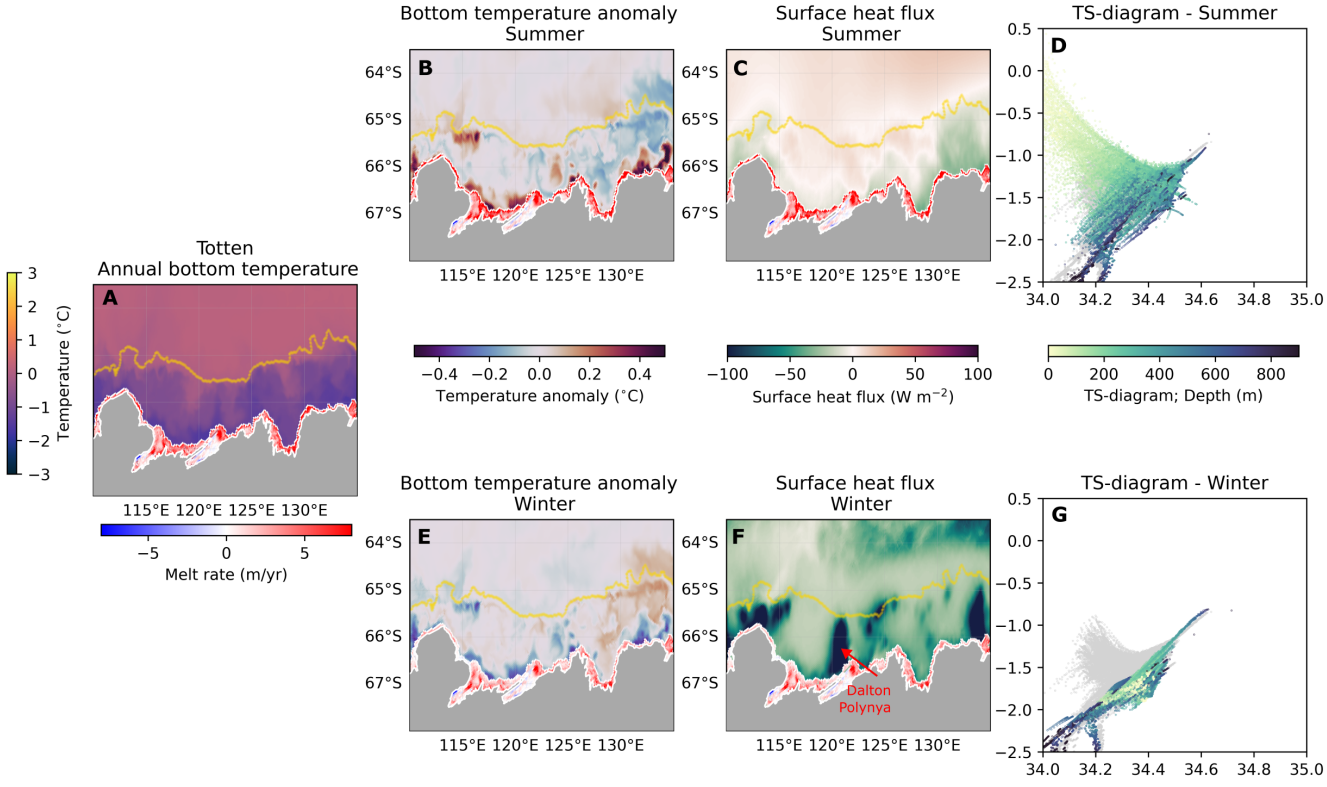

Figure 4. Maps in the Totten ice shelf region of (a) annual bottom temperature (over the last simulated year), (b) summer (January-May) mean bottom temperature anomaly, (c), summer mean surface heat flux, (e) winter (June-November) mean bottom temperature anomaly, and (f) winter mean surface heat flux. The 1500 m isobath is shown in yellow. Temperature-salinity diagrams with daily values along the ice shelf front for summer (d) and winter (g) averages; annual mean values are shown in gray. The basal melt rates are shown as annual mean (a), summer mean (b,c), and winter mean (e,f).

ing increased melting — a mechanism described as mode 3 (shallow) melting (Jacobs et al., 1992). In contrast, most of the West Antarctic can be classified as steady melting, mainly controlled by warm deep water inflow via deep troughs that does not have a strong seasonality (Walker et al., 2007, 2013). Although these warm intrusions exhibit high-frequency variability, likely associated with wind- and buoyancy-driven shelf circulation (Dotto et al., 2020; Yang et al., 2022), the heat supply is approximately constant, and seasonal variations are less pronounced.

These results indicate a dependency of ice shelf melt variability on the relative strength between melting modes. The seasonal melting regime at the Totten region is dictated by strong shallow melting, where seasonally warmed waters near the ice shelf front control most of the seasonal variability in basal melting. When CDW-driven melt dominates, as for the Getz region, the seasonal footprint of shallow melt becomes negligible. While Dense Shelf Water (DSW) has been associated with mode

https://doi.org/10.5194/egusphere-2024-3905
Preprint. Discussion started: 13 February 2025

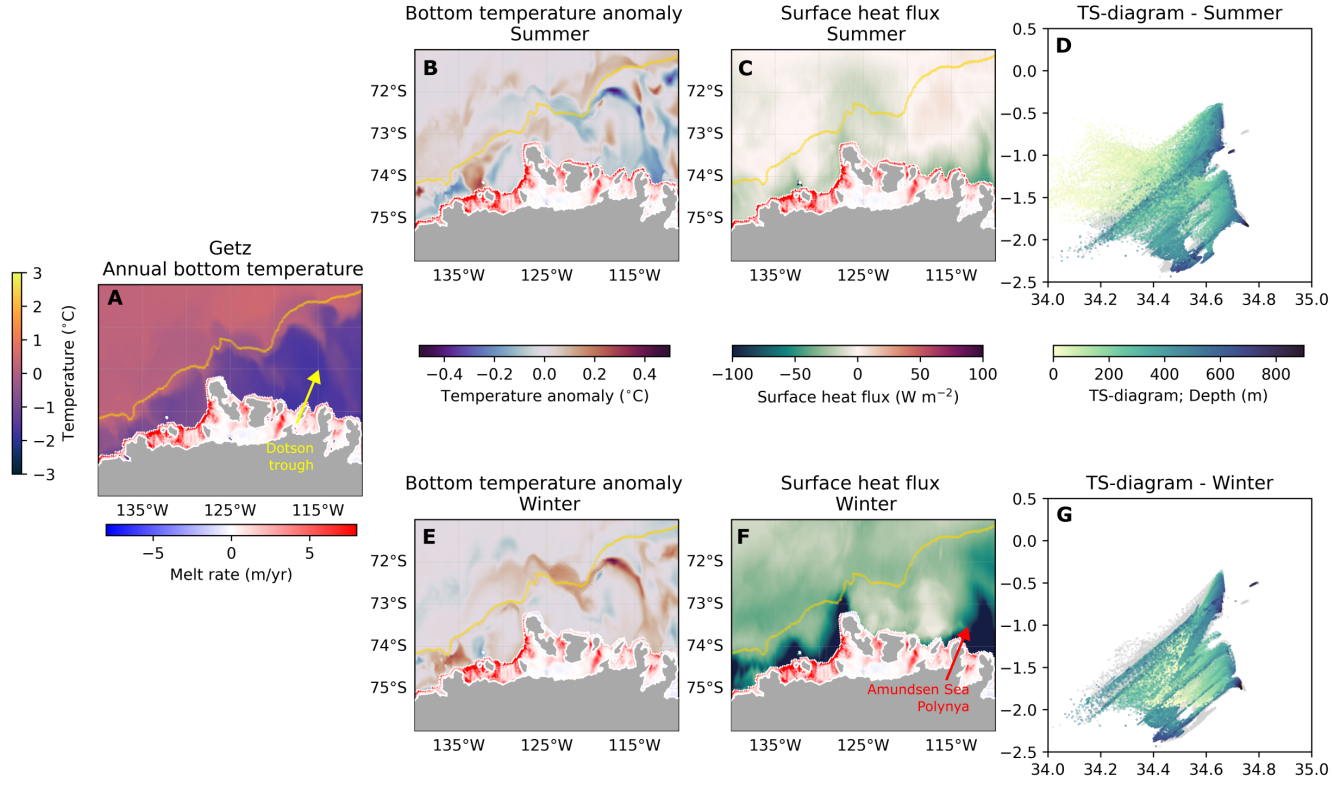

Figure 5. Maps in the Getz ice shelf region of (a) annual bottom temperature (over the last simulated year), (b) summer (January-May) mean bottom temperature anomaly, (c), summer mean surface heat flux, (e) winter (June-November) mean bottom temperature anomaly, and (f) winter mean surface heat flux. The 1500 m isobath is shown in yellow. Temperature-salinity diagrams with daily values along the ice shelf front for summer (d) and winter (g) averages; annual mean values are shown in gray. The basal melt rates are shown as annual mean (a), summer mean (b,c), and winter mean (e,f).

1 melt at large ice shelves (Nicholls et al., 2003) such as in the Filchner-Ronne Ice Shelf (Suppl. Material; Figures A5 and A8), our model shows that wintertime convection from coastal polynyas is important to cool down the ocean near the ice front region and actively interrupt the summertime increases in shallow melting.

We now discuss our circum-Antarctic model results in the context of previous studies. In the Sabrina Coast sector of East Antarctica, the Totten and Moscow University Ice Shelves buttress a marine ice sheet that holds ∼3.5 m of global mean sea level. Ground-based measurements show relatively low but highly variable melting of the Totten ice Shelf (Vaňková et al., 2021). These measurements are in agreement with regional modelling studies (e.g., Gwyther et al., 2014) but at some disagreement with satellite-based estimates that have shown melt peak rates (> 4 m yr^{-1}), comparable to those observed in the Amundsen and Bellingshausen Seas (Silvano et al., 2017). Although the Totten or Moscow University region is historically

https://doi.org/10.5194/egusphere-2024-3905
Preprint. Discussion started: 13 February 2025

under-sampled, previous modeling studies have shown the effect of coastal polynyas (i.e., Dalton Polynya) in modulating the basal melt variability (Gwyther et al., 2014; Khazendar et al., 2013; Kusahara et al., 2024), and recently the role of subglacial meltwater Gwyther et al. (2023), and intrinsic ocean variability that may also play a role here Gwyther et al. (2018); winds can also excerce an influence at longer (inter-annual) timescales (Greene et al., 2017). Coastal polynyas in this study are represented from observational estimates, giving confidence that the model captures relevant processes, such as the landfast ice effect on coastal polynya locations (Achter et al., 2022).

There is observational evidence of a seasonal cycle in basal melting in other parts of East Antarctica. In the Maud Land region, mode 3 (shallow) melting was observed in the Niulisen Ice Shelf (Lindbäck et al., 2019). Sun et al. (2019) also observed a seasonal pattern in basal melting under the Roi Baudouin Ice Shelf. In Prydz Bay, seasonality of warm intrusions has been identified from both observations and modelling (Galton-Fenzi et al., 2008; Gao et al., 2024), although here it is identified as mCDW inflow interrupted by polynyas in winter. Mode 3 has described melting underneath the Fimbul Ice Shelf from both observations and present-day simulations (Hattermann et al., 2012). In the Ross Ice Shelf, observations showed high melt variability associated with mode 3 melting (Stern et al., 2013; Arzeno et al., 2014; Kim et al., 2023) which has been associated with the Ross Sea Polynya (Stewart et al., 2019). Most of this observed seasonality points to similar mechanisms as described in our model.

In the West Antarctic, the Getz Ice Shelf produces more freshwater than any other ice shelf (Rignot et al., 2013; Jacobs et al., 2013) and influences the regional circulation in the Amundsen and Ross Seas (Nakayama et al., 2014). Accelerated thinning of the Getz has been observed since the 1990s (Paolo et al., 2015) and grounding line retreat since the 2000s (Christie et al., 2018), but lack of bathymetry and ocean measurements results in a poor understanding of the drivers of the Getz basal melting. More recent bathymetric measurements clarified the role of deep troughs under Getz in the CDW inflow to the ice shelf and also subglacial outflow for local melting increases (Wei et al., 2020). In our model, the basal melting at Getz is dominated by CDW-driven melting, with little seasonal variability (Assmann et al., 2019; Jacobs et al., 2013), and that weak polynya activity (and thus shelf cooling) allows for a constant supply of warm water via bottom layers (Silvano et al., 2018).

Several studies demonstrate that the Antarctic Ice Sheet mass loss observed in recent decades in the Amundsen Sea, West Antarctica (Rignot et al., 2013), is driven by warm water inflow causing ice shelf melting and thinning (Walker et al., 2007, 2013; Jacobs et al., 2011), responding in part to large-scale wind variability in the Pacific sector at inter-annual to decadal time scales (Adusumilli et al., 2020; Dotto et al., 2020; Yang et al., 2024) — although the remote drivers are still under debate (Park et al., 2024). Our model results, forced with a repeat year forcing, suggest that the majority of West Antarctic ice shelves have little seasonal variability (Figure 1d), implying that the melt variability is driven by longer timescales that may also be internally generated (e.g., Gwyther et al., 2018; Holland et al., 2019). Observational evidence of seasonality in the shelf circulation near the Dotson (Yang et al., 2022) and Pine Island ice shelves (Webber et al., 2017) exist and are also found in our model and in previous studies (Kimura et al., 2017). However, the seasonal variability is out-of-phase between these regions

https://doi.org/10.5194/egusphere-2024-3905
Preprint. Discussion started: 13 February 2025

and their magnitude are considerably smaller than the melt seasonality (Figure A4, middle panel), resulting in a substantially weaker seasonality than we found for East Antarctic ice shelves.

The Bellingshausen Sea is the only region which holds substantial differences across WAOM setups. At 10 km horizontal resolution, there is subtantially more CDW onshelf transport and basal melting than at 4 or 2 km resolution; see Dias et al. (2023) and Figure A3. The 10 km solution is closer to observations at this region (Schmidtko et al., 2014; Adusumilli et al., 2020), but it is important to note the Bellingshausen Sea region is comparatively much less observed than the Amundsen Sea (Christie et al., 2016). WAOM at 10 km shows particularly higher melting at the George VI Ice Shelf, which is dominated by CDW-driven melt and thus classified at steady melting regime, in contrast with the seasonal melting regime observed at 4 km due to cooler shelf and reduced CDW inflow (Figure 1b).

These results show how shallow melting can be a dominant source of basal melting variability at intra-annual timescales. This mode prevails in most of the East Antarctic ice shelves, from the eastern Ross to Fimbul and neighboring ice shelves. Our findings also point to the importance of the cooling effect of coastal polynyas to reduce melting near the ice shelf front during winter. In addition, summer warming (Antarctic Surface Waters formation) is concentrated near the icescape (ice shelf front, landfast ice or grounded icebergs), where most cooling takes place in the presence of local coastal polynyas or downstream, given the Antarctic Coastal Current influence (Liu et al., 2024). Given the importance of shallow melt (Jacobs et al., 1992) to basal melt variability, future scenarios where climate change could affect seasonal duration (Mosbeux et al., 2023), summer-time warming (Stewart et al., 2019), and coastal polynya activity (Kusahara et al., 2024) can cause large impacts on the melting of the ice shelves and for the buttressing of the Antarctic Ice Sheet. While previous studies indicate a shift between shallow melt to CDW-driven melt associated with future scenarios (Hattermann et al., 2014) and ongoing changes (Lauber et al., 2023), an intensification of shallow melting could enhance an extreme warming scenario (Kusahara et al., 2023), with potential large global sea-level impacts (Edwards et al., 2021; Seroussi et al., 2024).

Common to other modeling studies in such regions with very few observations and large uncertainties, the results described here have some limitations. WAOM has been shown to have cold biases in the West Antarctic and fresh biases in the Weddell Sea (Dias et al., 2023) relative to Schmidtko et al. (2014) , both associated with coastal polynya activity in these sectors that are captured in satellite estimates (Tamura et al., 2008) and contributes to local cooling and less CDW on-shelf intrusions. The choice of the repeat year forcing (2007) against a multi-decadal dataset (Schmidtko et al., 2014) is also likely contributing to the aforementioned differences. As coastal polynya location depends on the icescape, including grounded icebergs and fast ice (Cougnon et al., 2017; Achter et al., 2022) that are not captured in climate models (Heuzé, 2021; Dias et al., 2021), the basal melt estimates forced by CMIP5-6 models (Jourdain et al., 2022; Seroussi et al., 2024) will likely under-represent the polynyas' effect on melting near the ice front. Another important aspect is that WAOM does not include coupled sea-ice and so can overestimate the momentum (wind) effect on ocean currents (Jendersie et al., 2018). Surface wind sensitivity experiments using WAOM show this effect can be important in the West Antarctic sector, but there is less sensitivity in other regions (not

https://doi.org/10.5194/egusphere-2024-3905
Preprint. Discussion started: 13 February 2025

shown). The model's resolution, although relatively fine-scale for circumpolar standards, does not fully resolve eddy processes (Hallberg, 2013), in particular submesoscale eddies near the ice front, which could enhance shallow melting (Friedrichs et al., 2022). The model's vertical coordinates (terrain-following) needs to smooth sharp gradients and can misrepresent the ice shelf front (Naughten et al., 2018; Schnaase and Timmermann, 2019), with potential implications for shallow melting.

This study is the first circum-Antarctic description of the ocean processes driving basal melt at intra-annual timescales, and highlights the importance of shallow melting (Jacobs et al., 1992) to the seasonal variability as a dominant mechanism in the East Antarctic sector. Modelling studies such as undertaken here provide a unique opportunity to describe in detail the basal melting variability and the driving oceanic processes, which is essential to progress our understanding of ocean-ice shelf interactions given the lack of ocean measurements (Heywood et al., 2014) and bathymetry data along the Antarctic margin (Frémand et al., 2023). Recent studies have also highlighted that circum-Antarctic estimates of basal melting from satellites (e.g., Adusumilli et al., 2020) show large discrepancies from in-situ observations (Vaňková et al., 2021; Lindbäck et al., 2023), again suggesting modelling studies of the ocean processes around Antarctic ice shelves are essential to better understand the drivers of basal melting.

Our results highlight the importance of the seasonal Antarctic melting, modulated by the local icescape (i.e., coastal polynyas activity; Kusahara et al. 2010), to the basal melt variability in a present-day scenario. Climate change-induced impacts on seasonality (Timmermann and Goeller, 2017; Mosbeux et al., 2023) and sea-ice regime (Purich and Doddridge, 2023), in particular affected by anomalous summertime atmospheric conditions in association with stronger positive Southern Annular Mode phase (Clem et al., 2024), can have potentially large implications for shallow melting and thus to Antarctic Ice Sheet mass loss and global sea level rise.

Code and data availability. All the post-processing scripts used in this study are freely available in https://github.com/fabiobdias/waom_notebook. The model outputs are available from the corresponding author on request.

Appendix A: Appendix A

https://doi.org/10.5194/egusphere-2024-3905
Preprint. Discussion started: 13 February 2025

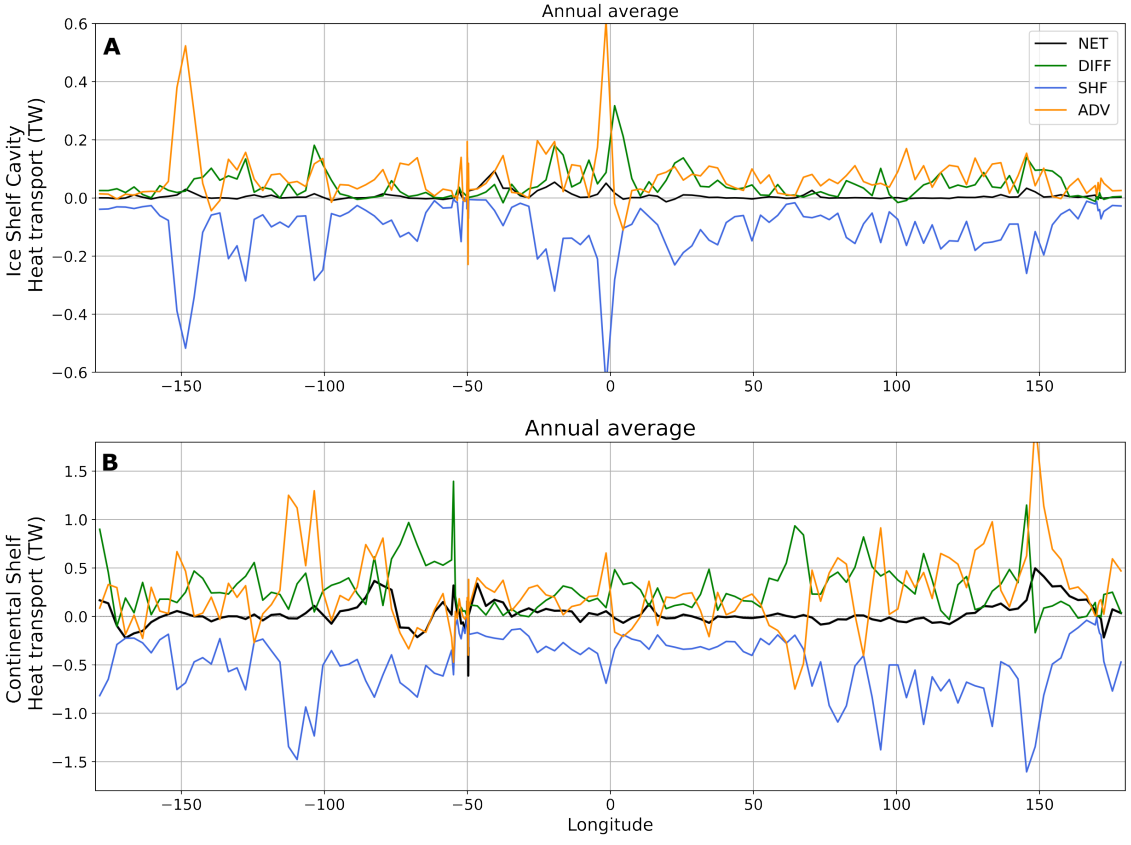

Figure A1. As in Figure 2 but for the annual mean ocean heat budget horizontally- and vertically-integrated over longitudinal bins (in TW) for the whole continental shelf (including ice shelf cavities, upper panel) and only the ice shelf cavities (lower panel).

https://doi.org/10.5194/egusphere-2024-3905
Preprint. Discussion started: 13 February 2025

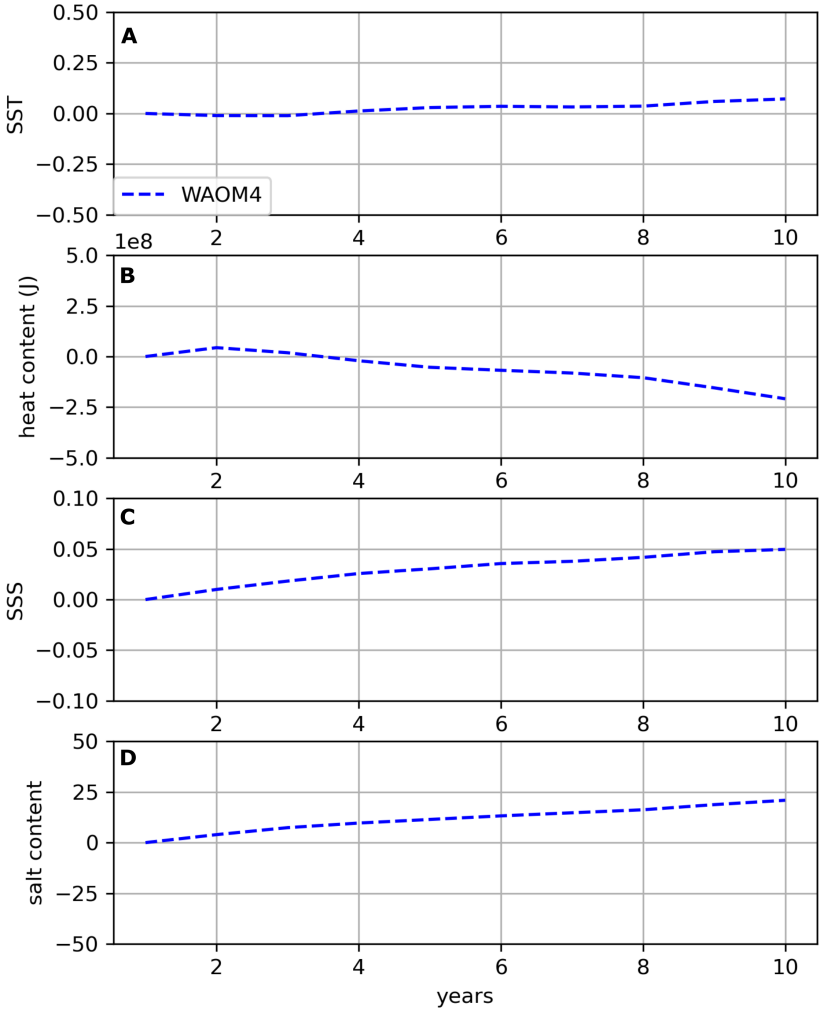

Figure A2. Evolution over the 10-years simulation of the shelf integrated (south of the 1500 m isobath) for (a) sea surface temperature (SST, in °C), (b) ocean heat content (Joules), (c) sea surface salinity (SSS), and (d) ocean salt content.

https://doi.org/10.5194/egusphere-2024-3905
Preprint. Discussion started: 13 February 2025

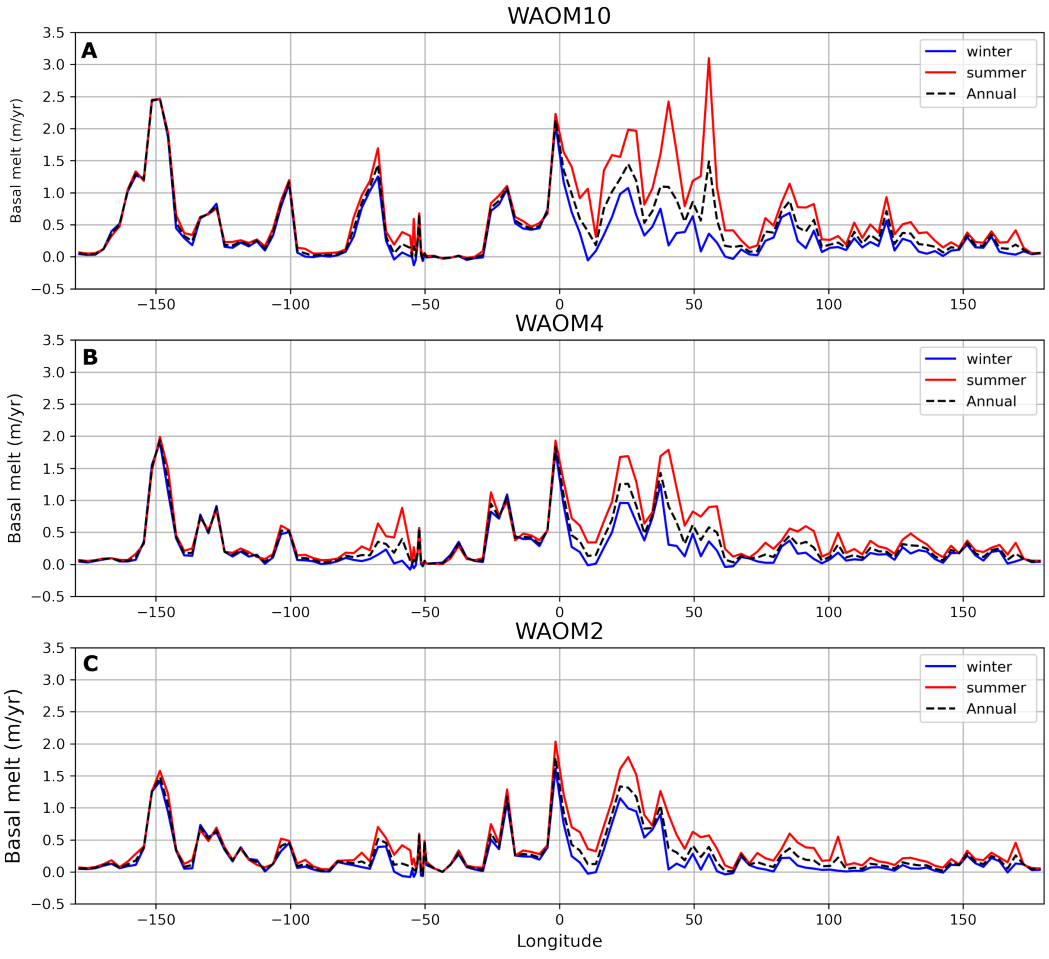

Figure A3. Basal melt rates integrated over each longitudinal bin (Gt/yr, 1 Gt = $1x10^{12}$ kg) for WAOM10 (10 km horizontal resolution), WAOM4 and WAOM2, shown as annual (black dashed line), January-March (yellow), April-June (blue), July-September (red) and October-December (magenta).

https://doi.org/10.5194/egusphere-2024-3905
Preprint. Discussion started: 13 February 2025

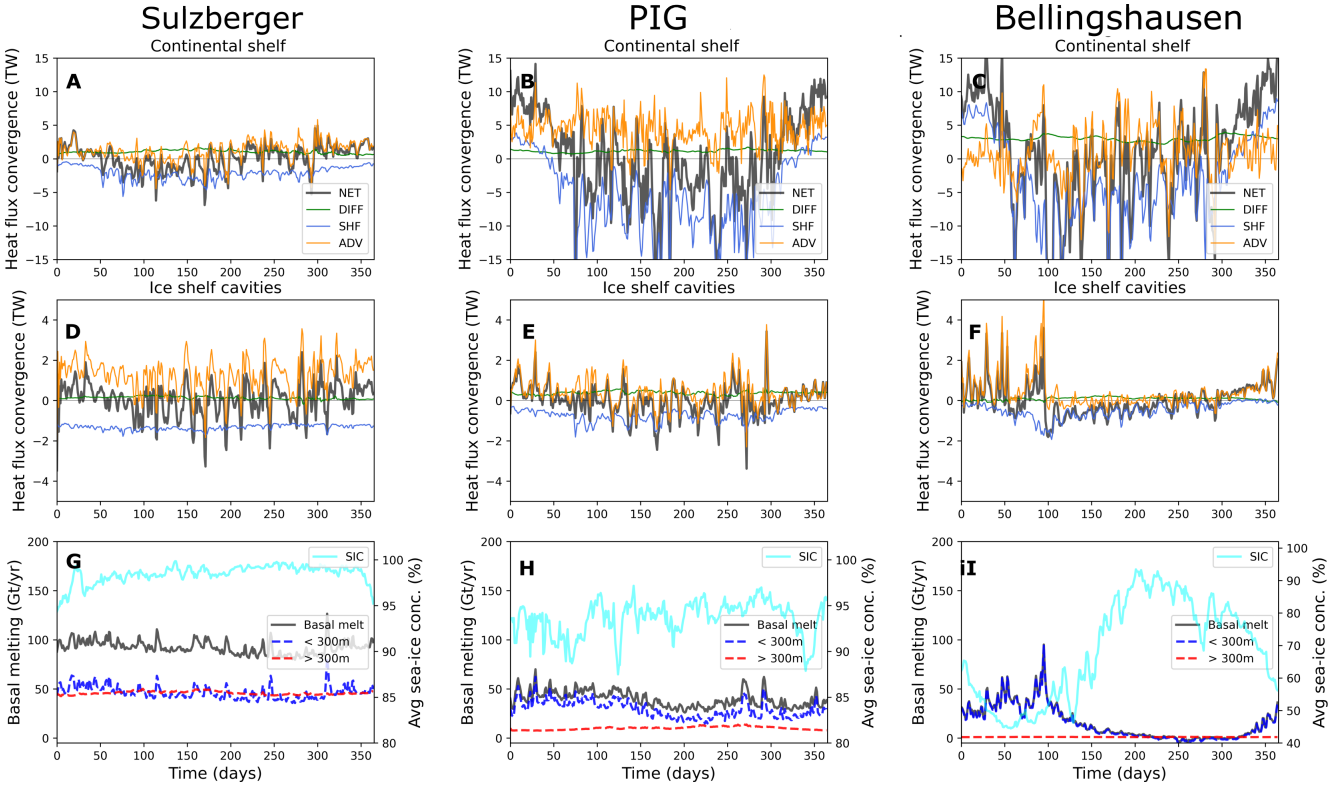

Figure A4. As in Figure 3 but showing ocean heat budget (OHB) horizontally- and vertically-integrated over the vicinity of the Sulzberger Ice Shelf (left column), Pine-Island Ice Shelf (middle column) and the Bellingshausen Sea region (right column).

https://doi.org/10.5194/egusphere-2024-3905
Preprint. Discussion started: 13 February 2025

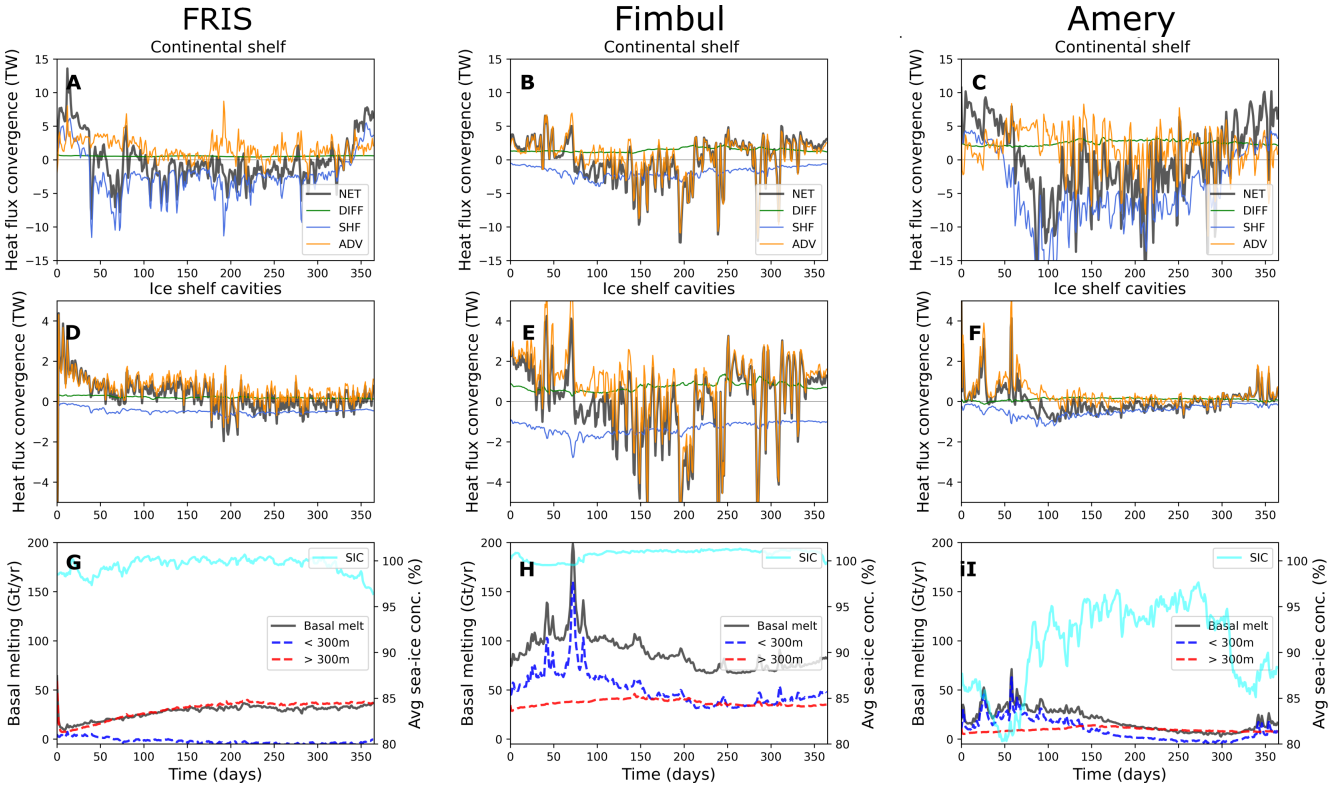

Figure A5. As in Figure 3, but showing ocean heat budget (OHB) horizontally- and vertically-integrated over the vicinity of the Filchner-Ronne Ice Shelf (left column), Fimbul Ice Shelf (middle column) and Amery Ice Shelf region (right column).

https://doi.org/10.5194/egusphere-2024-3905
Preprint. Discussion started: 13 February 2025

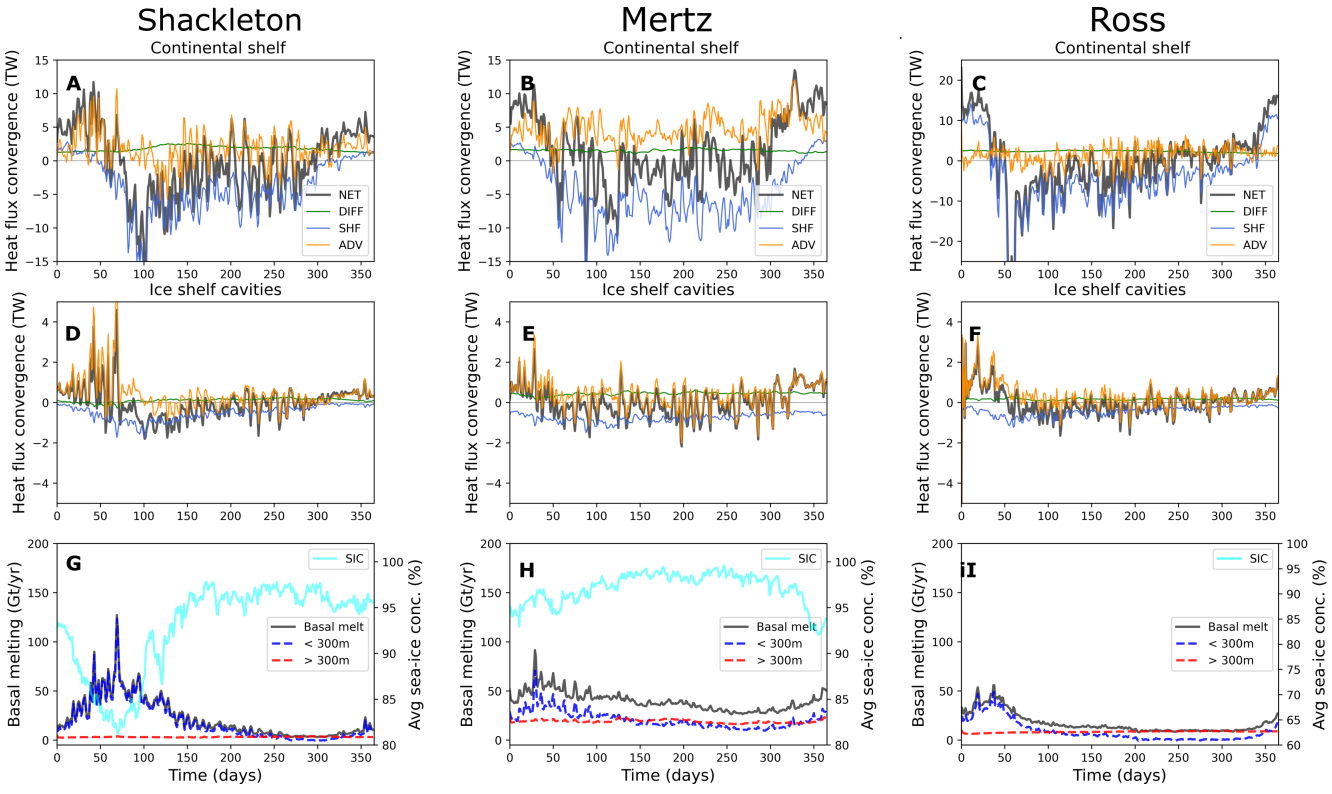

Figure A6. As in Figure 3), ocean heat budget (OHB) horizontally- and vertically-integrated over the vicinity of the Shackleton Ice Shelf (left column), Mertz Ice Shelf (middle column) and Ross Ice Shelf region (right column).

https://doi.org/10.5194/egusphere-2024-3905
Preprint. Discussion started: 13 February 2025

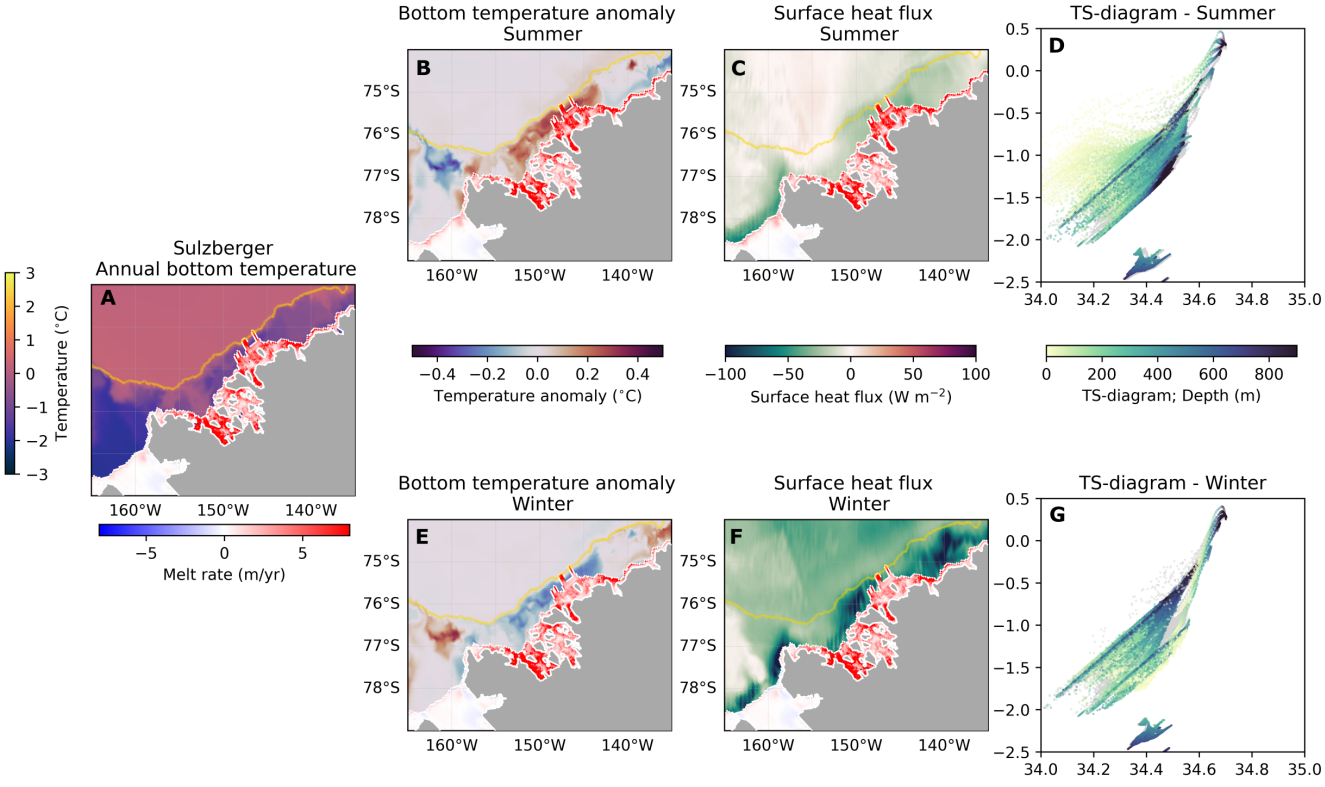

Figure A7. As in Figure 4 but for the Sulzberger ice shelf region.

Author contributions. FBD, AKM, BGF and MHE conceived the study. FBD configured and ran the model simulations, performed the diagnostic analyses, and wrote the paper. All authors discussed the results and reviewed the manuscript draft.

Competing interests. The contact author has declared that none of the authors has any competing interests.

Acknowledgements. This research was undertaken on the National Computational Infrastructure (NCI) in Canberra, Australia, which is supported by the Australian Government. This research was supported by the ARC Australian Centre for Excellence in Antarctic Science (ACEAS; AProject SR200100008), ARC Discovery Project DP190100494 and DP250100759.

https://doi.org/10.5194/egusphere-2024-3905
Preprint. Discussion started: 13 February 2025

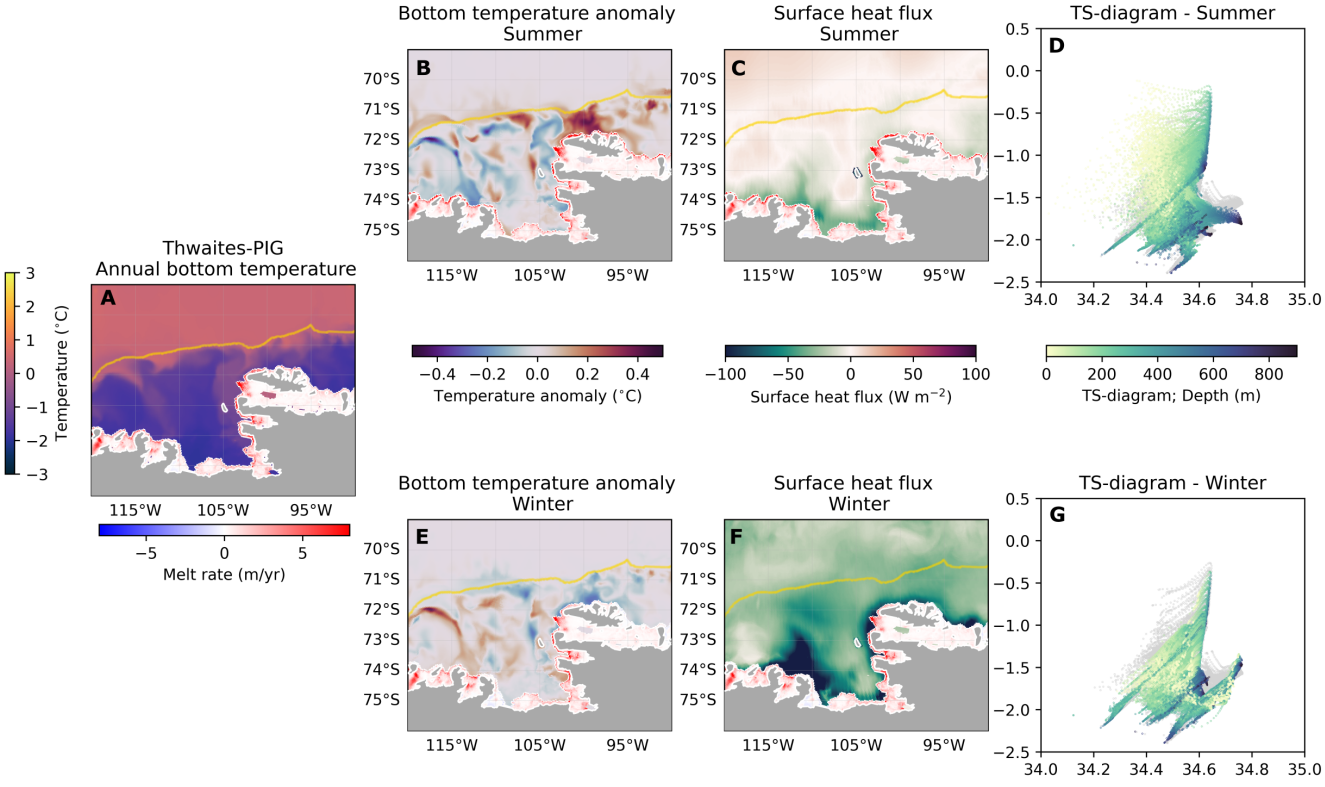

Figure A8. As in Figure 4 but for the Pine Island ice shelf region.

References

https://doi.org/10.5194/egusphere-2024-3905
Preprint. Discussion started: 13 February 2025

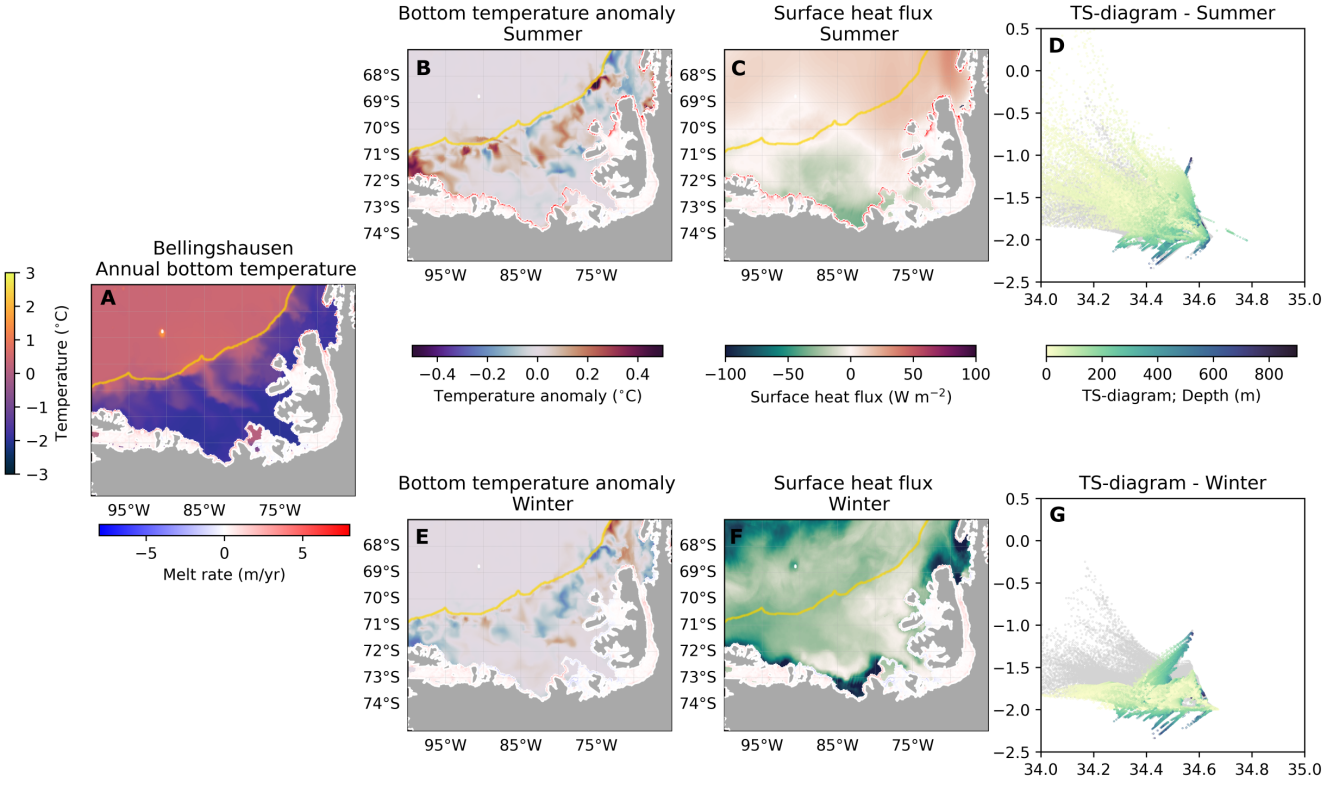

Figure A9. As in Figure 4 but for the Bellingshausen Sea region.

References

Achter, G. V., Fichefet, T., Goosse, H., Pelletier, C., Sterlin, J., Huot, P. V., Lemieux, J. F., Fraser, A. D., Haubner, K., and Porter-Smith, R.: Modelling landfast sea ice and its influence on ocean–ice interactions in the area of the Totten Glacier, East Antarctica, Ocean Modelling, 169, https://doi.org/10.1016/j.ocemod.2021.101920, 2022.

Adusumilli, S., Fricker, H. A., Medley, B., Padman, L., and Siegfried, M. R.: Interannual variations in meltwater input to the Southern Ocean from Antarctic ice shelves, Nature Geoscience, 13, 616–620, https://doi.org/10.1038/s41561-020-0616-z, 2020.

Alley, K. E., Scambos, T. A., Siegfried, M. R., and Fricker, H. A.: Impacts of warm water on Antarctic ice shelf stability through basal channel formation, Nature Geoscience, 9, 290–293, https://doi.org/10.1038/ngeo2675, 2016.

Arzeno, I. B., Beardsley, R. C., Limeburner, R., Owens, B., Padman, L., Springer, S. R., Stewart, C. L., and Williams, M. J.: Ocean variability contributing to basal melt rate near the ice front of Ross Ice Shelf, Antarctica, Journal of Geophysical Research: Oceans, 119, 4214–4233, https://doi.org/10.1002/2014JC009792, 2014.

Assmann, K. M., Darelius, E., Wåhlin, A. K., Kim, T. W., and Lee, S. H.: Warm Circumpolar Deep Water at the Western Getz Ice Shelf Front, Antarctica, Geophysical Research Letters, 46, 870–878, https://doi.org/10.1029/2018GL081354, 2019.

https://doi.org/10.5194/egusphere-2024-3905
Preprint. Discussion started: 13 February 2025

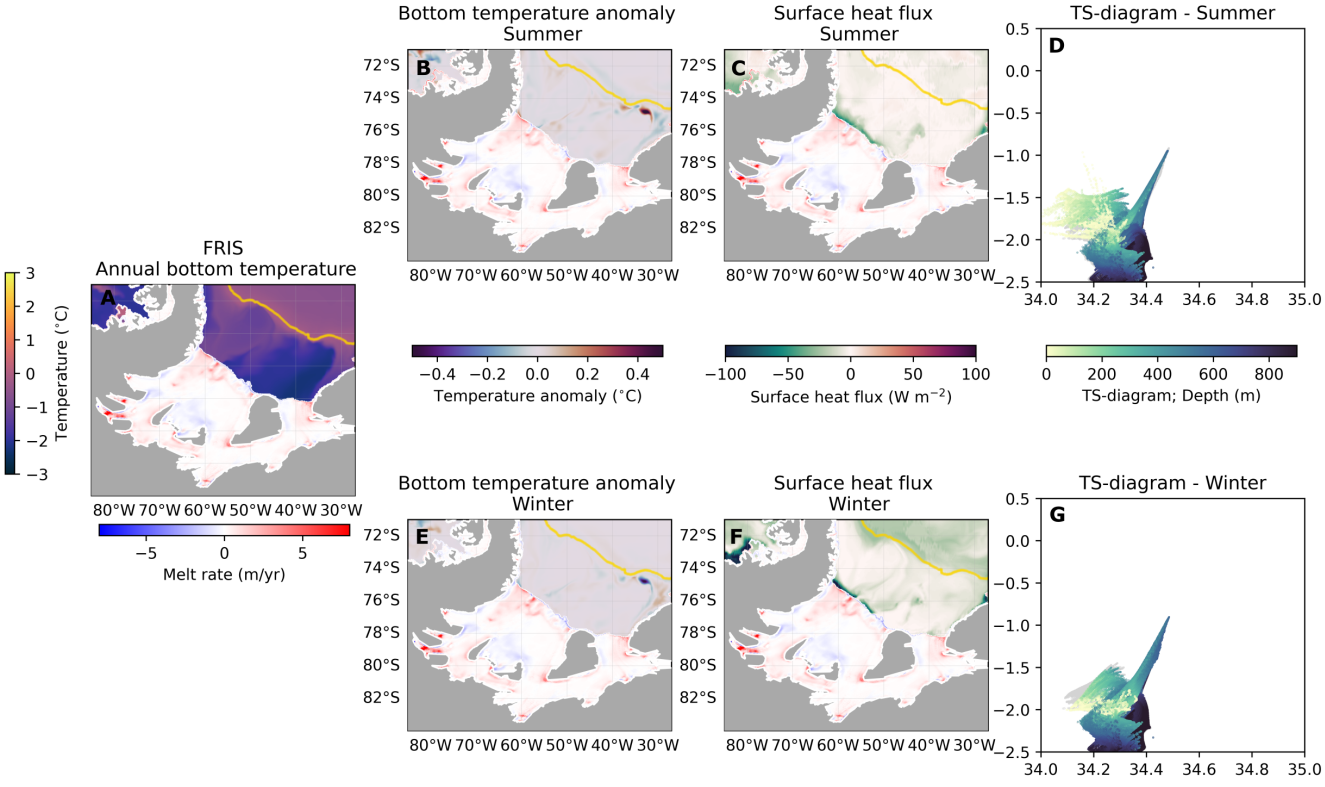

Figure A10. As in Figure 4 but for the Filchner-Ronne ice shelf region.

Christie, F. D., Bingham, R. G., Gourmelen, N., Tett, S. F., and Muto, A.: Four-decade record of pervasive grounding line retreat along the Bellingshausen margin of West Antarctica, https://doi.org/10.1002/2016GL068972, 2016.

Christie, F. D., Bingham, R. G., Gourmelen, N., Steig, E. J., Bisset, R. R., Pritchard, H. D., Snow, K., and Tett, S. F.: Glacier change along West Antarctica's Marie Byrd Land Sector and links to inter-decadal atmosphere-ocean variability, Cryosphere, 12, 2461–2479, https://doi.org/10.5194/tc-12-2461-2018, 2018.

Clem, K. R., Raphael, M. N., Adusumilli, S., Amory, C., Baiman, R., Banwell, A. F., Barreira, S., Beadling, R. L., Bozkurt, D., Colwell, S., Coy, L., Datta, R. T., Deb, P., Laat, J. D., du Plessis, M., Fernandez, D., Fogt, R. L., Fricker, H. A., Gille, S. T., Johnson, B., Josey, S. A., Keller, L. M., Kramarova, N. A., Kromer, J., Leslie, R. L., Lazzara, M. A., Lieser, J. L., MacFerrin, M., MacGilchrist, G. M., MacLennan, M. L., Marouchos, A., Massom, R. A., McMahon, C. R., Mikolajczyk, D. E., Mote, T. L., Newman, P. A., Norton, T., Petropavlovskikh, I., Pezzi, L. P., Pitts, M., Reid, P., Santee, M. L., Scambos, T. A., Schulz, C., Shi, J.-R., Souza, E., Stammerjohn, S., Thomalla, S., Tripathy, S. C., Trusel, L. D., Turner, K., and Yin, Z.: Antarctica and the Southern Ocean, Bulletin of the American Meteorological Society, 105, S331–S370, https://doi.org/10.1175/BAMS-D-24-0099.1, 2024.

Cook, S., Nicholls, K. W., Vaňková, I., Thompson, S. S., and Galton-Fenzi, B. K.: Data initiatives for ocean-driven melt of Antarctic ice shelves, Annals of Glaciology, 45, https://doi.org/10.1017/aog.2023.6, 2023.

https://doi.org/10.5194/egusphere-2024-3905
Preprint. Discussion started: 13 February 2025

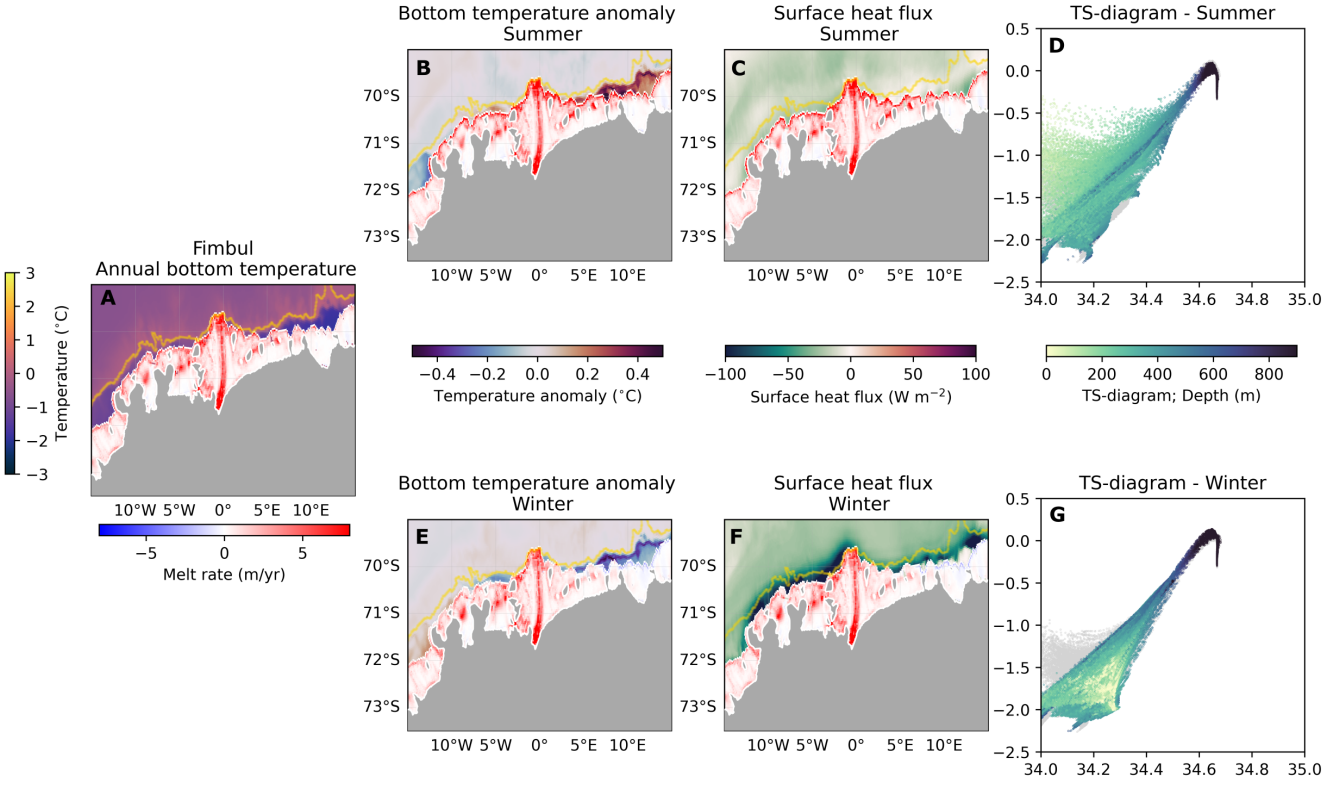

Figure A11. As in Figure 4 but for the Fimbul ice shelf region.

Cougnon, E. A., Galton-Fenzi, B. K., Rintoul, S. R., Legrésy, B., Williams, G. D., Fraser, A. D., and Hunter, J. R.: Regional Changes in Icescape Impact Shelf Circulation and Basal Melting, Geophysical Research Letters, 44, 11,519–11,527, https://doi.org/10.1002/2017GL074943, 2017.

Davis, P. E., Jenkins, A., Nicholls, K. W., Brennan, P. V., Abrahamsen, E. P., Heywood, K. J., Dutrieux, P., Cho, K. H., and Kim, T. W.: Variability in Basal Melting Beneath Pine Island Ice Shelf on Weekly to Monthly Timescales, Journal of Geophysical Research: Oceans, 123, 8655–8669, https://doi.org/10.1029/2018JC014464, 2018.

Dee, D. P., Uppala, S. M., Simmons, A. J., Berrisford, P., Poli, P., Kobayashi, S., Andrae, U., Balmaseda, M. A., Balsamo, G., Bauer, P., Bechtold, P., Beljaars, A. C., van de Berg, L., Bidlot, J., Bormann, N., Delsol, C., Dragani, R., Fuentes, M., Geer, A. J., Haimberger, L., Healy, S. B., Hersbach, H., Hólm, E. V., Isaksen, L., Kållberg, P., Köhler, M., Matricardi, M., Mcnally, A. P., Monge-Sanz, B. M., Morcrette, J. J., Park, B. K., Peubey, C., de Rosnay, P., Tavolato, C., Thépaut, J. N., and Vitart, F.: The ERA-Interim reanalysis: Configuration and performance of the data assimilation system, Quarterly Journal of the Royal Meteorological Society, 137, 553–597, https://doi.org/10.1002/qj.828, 2011.

Dias, F. B., Domingues, C. M., Marsland, S. J., Rintoul, S. R., Uotila, P., Fiedler, R., Mata, M. M., Bindoff, N. L., and Savita, A.: Subpolar Southern Ocean Response to Changes in the Surface Momentum, Heat, and Freshwater Fluxes under 2xCO2, Journal of Climate, 34, 8755–8775, https://doi.org/10.1175/JCLI-D-21-0161.1, 2021.

https://doi.org/10.5194/egusphere-2024-3905
Preprint. Discussion started: 13 February 2025

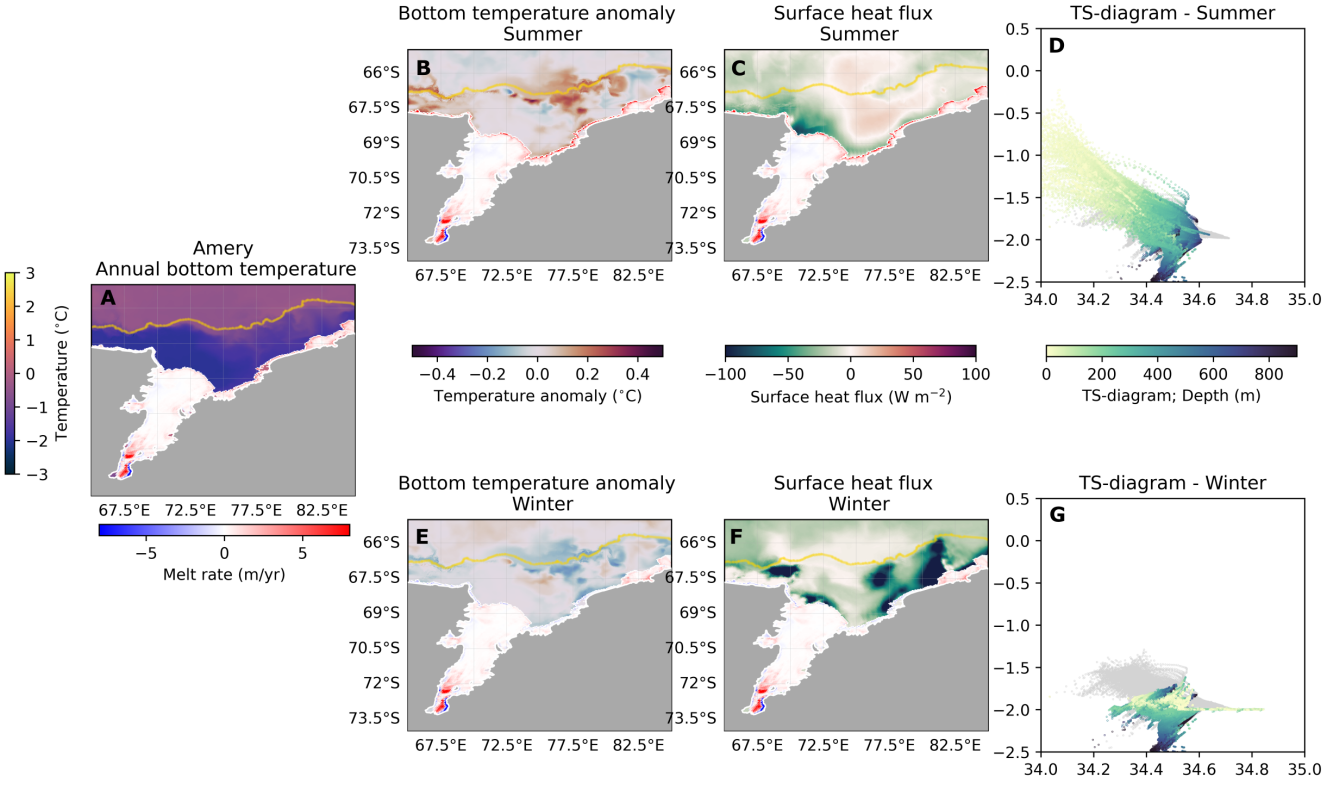

Figure A12. As in Figure 4 but for the Amery ice shelf region.

Dias, F. B., Rintoul, S. R., Richter, O., Galton-Fenzi, B. K., Zika, J. D., Pellichero, V., and Uotila, P.: Sensitivity of simulated water mass transformation on the Antarctic shelf to tides, topography and model resolution, Frontiers in Marine Science, 10, https://doi.org/10.3389/fmars.2023.1027704, 2023.

Dinniman, M. S., Klinck, J. M., and Smith, W. O.: Influence of sea ice cover and icebergs on circulation and water mass formation in a numerical circulation model of the Ross Sea, Antarctica, Journal of Geophysical Research: Oceans, 112, https://doi.org/10.1029/2006JC004036, 2007.

Dotto, T. S., Garabato, A. C. N., Wåhlin, A. K., Bacon, S., Holland, P. R., Kimura, S., Tsamados, M., Herraiz-Borreguero, L., Kalén, O., and Jenkins, A.: Control of the Oceanic Heat Content of the Getz-Dotson Trough, Antarctica, by the Amundsen Sea Low, Journal of Geophysical Research: Oceans, 125, https://doi.org/10.1029/2020JC016113, 2020.

Drews, R.: Evolution of ice-shelf channels in Antarctic ice shelves, Cryosphere, 9, 1169–1181, https://doi.org/10.5194/tc-9-1169-2015, 2015.

Edwards, T. L., Nowicki, S., Marzeion, B., Hock, R., Goelzer, H., Seroussi, H., Jourdain, N. C., Slater, D. A., Turner, F. E., Smith, C. J., McKenna, C. M., Simon, E., Abe-Ouchi, A., Gregory, J. M., Larour, E., Lipscomb, W. H., Payne, A. J., Shepherd, A., Agosta, C., Alexander, P., Albrecht, T., Anderson, B., Asay-Davis, X., Aschwanden, A., Barthel, A., Bliss, A., Calov, R., Chambers, C., Champollion, N., Choi, Y., Cullather, R., Cuzzone, J., Dumas, C., Felikson, D., Fettweis, X., Fujita, K., Galton-Fenzi, B. K., Gladstone,

https://doi.org/10.5194/egusphere-2024-3905
Preprint. Discussion started: 13 February 2025

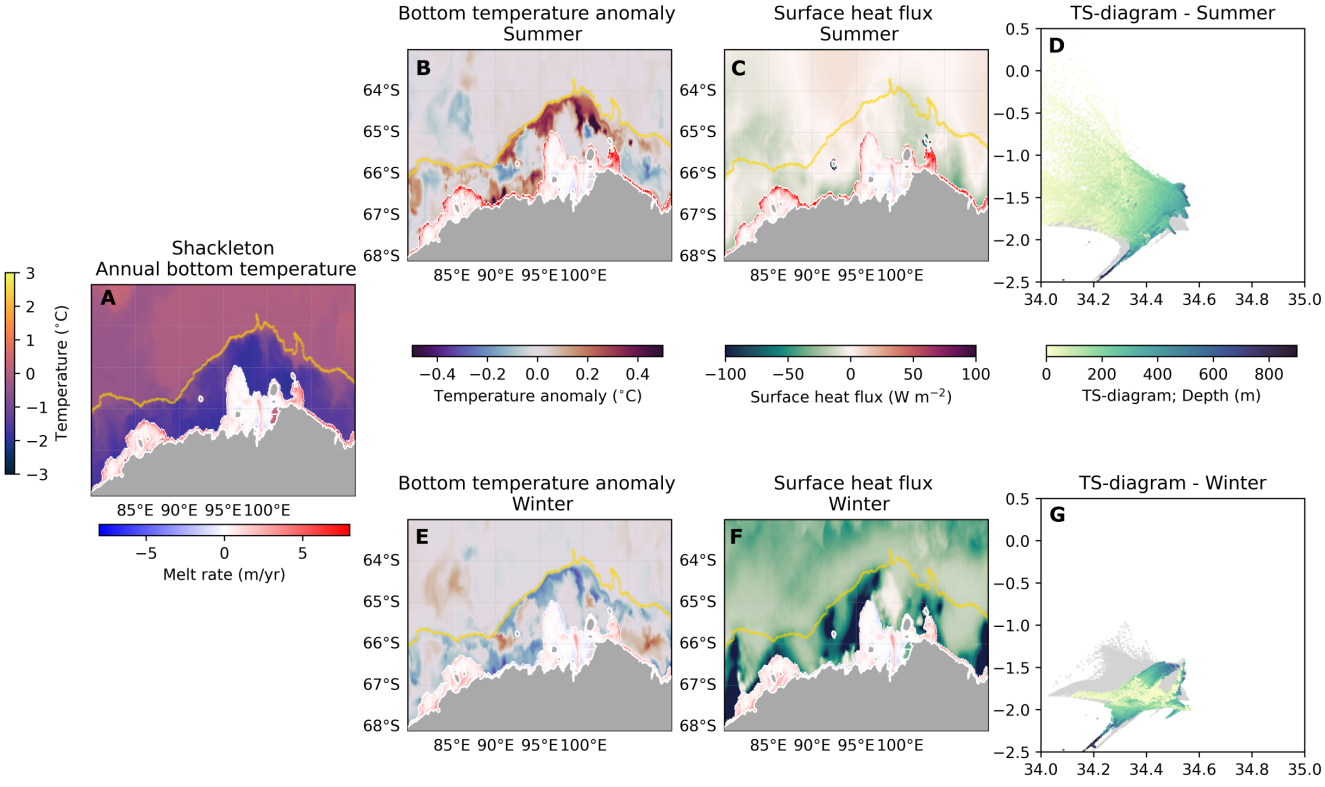

Figure A13. As in Figure 4 but for the Shackleton ice shelf region.

R., Golledge, N. R., Greve, R., Hattermann, T., Hoffman, M. J., Humbert, A., Huss, M., Huybrechts, P., Immerzeel, W., Kleiner, T., Kraaijenbrink, P., clec'h, S. L., Lee, V., Leguy, G. R., Little, C. M., Lowry, D. P., Malles, J. H., Martin, D. F., Maussion, F., Morlighem, M., O'Neill, J. F., Nias, I., Pattyn, F., Pelle, T., Price, S. F., Quiquet, A., Radić, V., Reese, R., Rounce, D. R., Rückamp, M., Sakai, A., Shafer, C., Schlegel, N. J., Shannon, S., Smith, R. S., Straneo, F., Sun, S., Tarasov, L., Trusel, L. D., Breedam, J. V., van de Wal, R., van den Broeke, M., Winkelmann, R., Zekollari, H., Zhao, C., Zhang, T., and Zwinger, T.: Projected land ice contributions to twenty-first-century sea level rise, Nature, 593, 74–82, https://doi.org/10.1038/s41586-021-03302-y, 2021.

Egbert, G. D. and Erofeeva, S. Y.: Efficient Inverse Modeling of Barotropic Ocean Tides, 2002.

Fox-Kemper, B., Hewitt, H., Xiao, C., Aðalgeirsdótti, G., Drijfhout, S., Edwards, T., Golledge, M. H. N., Kopp, R., Krinner, G., Mix, D. N. A., Nowicki, S., Nurhati, I., Ruiz, L., Sallée, J.-B., Slangen, A., and Yu, Y.: Ocean, Cryosphere and Sea Level Change, https://doi.org/10.1017/9781009157896.011, 2023.

Fraser, A. D., Wongpan, P., Langhorne, P. J., Klekociuk, A. R., Kusahara, K., Lannuzel, D., Massom, R. A., Meiners, K. M., Swadling, K. M., Atwater, D. P., Brett, G. M., Corkill, M., Dalman, L. A., Fiddes, S., Granata, A., Guglielmo, L., Heil, P., Leonard, G. H., Mahoney, A. R., McMinn, A., van der Merwe, P., Weldrick, C. K., and Wienecke, B.: Antarctic Landfast Sea Ice: A Review of Its Physics, Biogeochemistry and Ecology, https://doi.org/10.1029/2022RG000770, 2023.

https://doi.org/10.5194/egusphere-2024-3905
Preprint. Discussion started: 13 February 2025

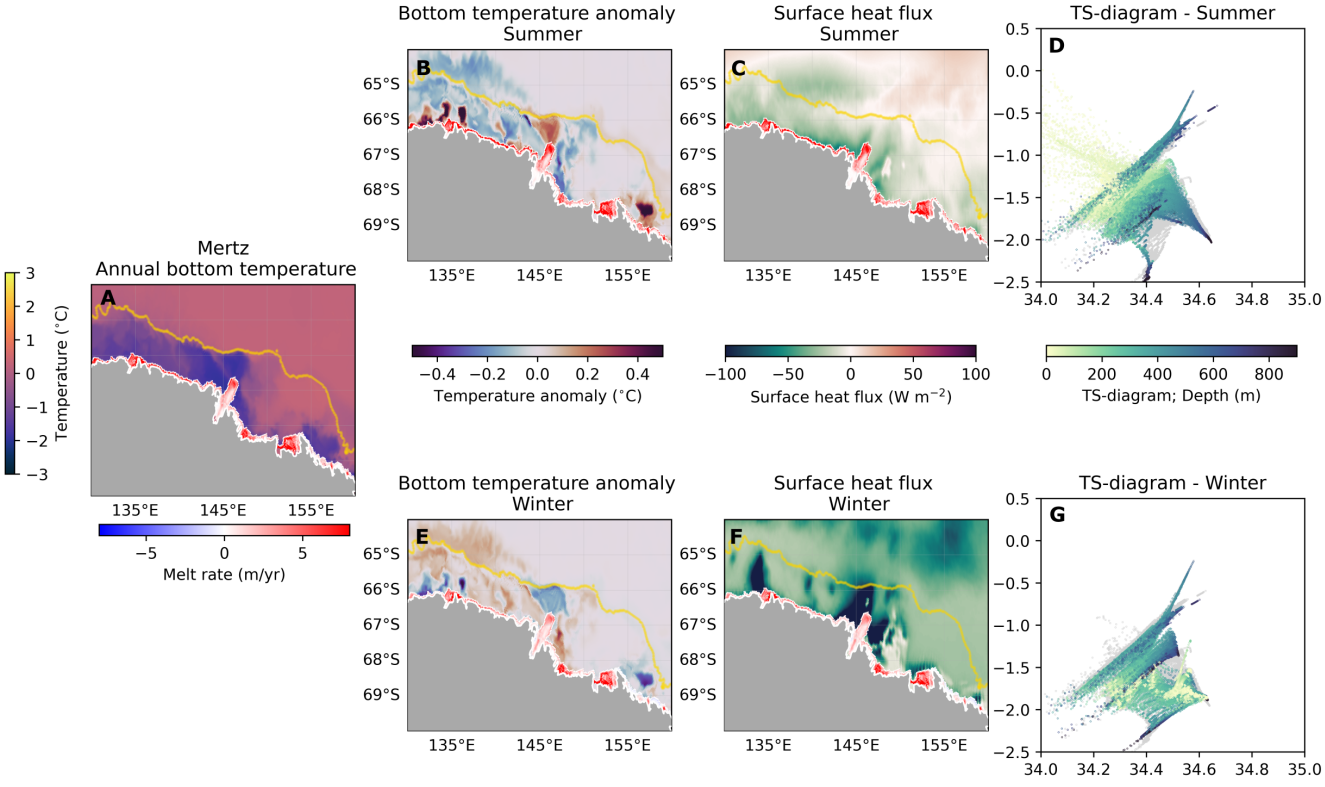

Figure A14. As in Figure 4 but for the Mertz ice shelf region.

Fretwell, P., Pritchard, H. D., Vaughan, D. G., Bamber, J. L., Barrand, N. E., Bell, R., Bianchi, C., Bingham, R. G., Blankenship, D. D., Casassa, G., Catania, G., Callens, D., Conway, H., Cook, A. J., Corr, H. F., Damaske, D., Damm, V., Ferraccioli, F., Forsberg, R., Fujita, S., Gim, Y., Gogineni, P., Griggs, J. A., Hindmarsh, R. C., Holmlund, P., Holt, J. W., Jacobel, R. W., Jenkins, A., Jokat, W., Jordan, T., King, E. C., Kohler, J., Krabill, W., Riger-Kusk, M., Langley, K. A., Leitchenkov, G., Leuschen, C., Luyendyk, B. P., Matsuoka, K., Mouginot, J., Nitsche, F. O., Nogi, Y., Nost, O. A., Popov, S. V., Rignot, E., Rippin, D. M., Rivera, A., Roberts, J., Ross, N., Siegert, M. J., Smith, A. M., Steinhage, D., Studinger, M., Sun, B., Tinto, B. K., Welch, B. C., Wilson, D., Young, D. A., Xiangbin, C., and Zirizzotti, A.: Bedmap2: Improved ice bed, surface and thickness datasets for Antarctica, Cryosphere, 7, 375–393, https://doi.org/10.5194/tc-7-375-2013, 2013.

Friedrichs, D. M., McInerney, J. B., Oldroyd, H. J., Lee, W. S., Yun, S., Yoon, S. T., Stevens, C. L., Zappa, C. J., Dow, C. F., Mueller, D., Steiner, O. S., and Forrest, A. L.: Observations of submesoscale eddy-driven heat transport at an ice shelf calving front, Communications Earth and Environment, 3, https://doi.org/10.1038/s43247-022-00460-3, 2022.

Frémand, A. C., Fretwell, P., Bodart, J. A., Pritchard, H. D., Aitken, A., Bamber, J. L., Bell, R., Bianchi, C., Bingham, R. G., Blankenship, D. D., Casassa, G., Catania, G., Christianson, K., Conway, H., Corr, H. F. J., Cui, X., Damaske, D., Damm, V., Drews, R., Eagles, G., Eisen, O., Eisermann, H., Ferraccioli, F., Field, E., Forsberg, R., Franke, S., Fujita, S., Gim, Y., Goel, V., Gogineni, S. P., Greenbaum, J., Hills, B., Hindmarsh, R. C. A., Hoffman, A. O., Holmlund, P., Holschuh, N., Holt, J. W., Horlings, A. N., Humbert, A., Jacobel, R. W.,

https://doi.org/10.5194/egusphere-2024-3905
Preprint. Discussion started: 13 February 2025

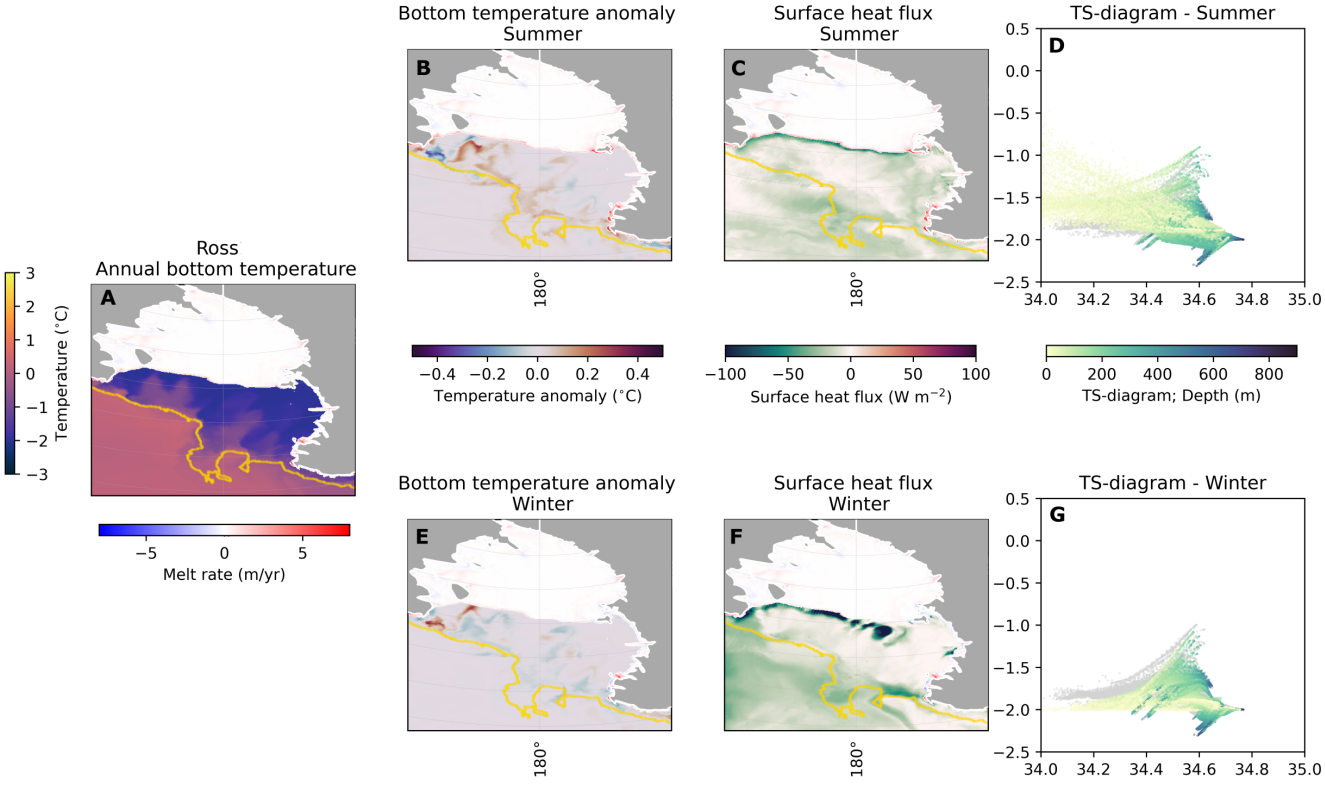

Figure A15. As in Figure 4 but for the Ross ice shelf region.

Jansen, D., Jenkins, A., Jokat, W., Jordan, T., King, E., Kohler, J., Krabill, W., Gillespie, M. K., Langley, K., Lee, J., Leitchenkov, G., Leuschen, C., Luyendyk, B., MacGregor, J., MacKie, E., Matsuoka, K., Morlighem, M., Mouginot, J., Nitsche, F. O., Nogi, Y., Nost, O. A., Paden, J., Pattyn, F., Popov, S. V., Rignot, E., Rippin, D. M., Rivera, A., Roberts, J., Ross, N., Ruppel, A., Schroeder, D. M., Siegert, M. J., Smith, A. M., Steinhage, D., Studinger, M., Sun, B., Tabacco, I., Tinto, K., Urbini, S., Vaughan, D., Welch, B. C., Wilson, D. S., Young, D. A., and Zirizzotti, A.: Antarctic Bedmap data: Findable, Accessible, Interoperable, and Reusable (FAIR) sharing of 60 years of ice bed, surface, and thickness data, Earth System Science Data, 15, 2695–2710, https://doi.org/10.5194/essd-15-2695-2023, 2023.

Galton-Fenzi, B., Maraldi, C., Coleman, R., and Hunter, J.: The cavity under the Amery Ice Shelf, East Antarctica, Journal of Glaciology, 54, 881–887, https://doi.org/hal-00406802v1, 2008.

Galton-Fenzi, B. K., Hunter, J. R., Coleman, R., Marsland, S. J., and Warner, R. C.: Modeling the basal melting and marine ice accretion of the Amery Ice Shelf, Journal of Geophysical Research: Oceans, 117, https://doi.org/10.1029/2012JC008214, 2012.

https://doi.org/10.5194/egusphere-2024-3905
Preprint. Discussion started: 13 February 2025

Gao, L., Yuan, X., Cai, W., Guo, G., Yu, W., Shi, J., Qiao, F., Wei, Z., and Williams, G. D.: Persistent warm-eddy transport to Antarctic ice shelves driven by enhanced summer westerlies, Nature Communications, 15, https://doi.org/10.1038/s41467-024-45010-x, 2024.

Greene, C. A., Blankenship, D. D., Gwyther, D. E., Silvano, A., and van Wijk, E.: Wind causes Totten Ice Shelf melt and acceleration, Science Advances, 3, https://doi.org/10.1126/sciadv.1701681, 2017.

Gwyther, D. E., Galton-Fenzi, B. K., Hunter, J. R., and Roberts, J. L.: Simulated melt rates for the Totten and Dalton ice shelves, Ocean Science, 10, 267–279, https://doi.org/10.5194/os-10-267-2014, 2014.

Gwyther, D. E., O'Kane, T. J., Galton-Fenzi, B. K., Monselesan, D. P., and Greenbaum, J. S.: Intrinsic processes drive variability in basal melting of the Totten Glacier Ice Shelf, Nature Communications, 9, https://doi.org/10.1038/s41467-018-05618-2, 2018.

Gwyther, D. E., Dow, C. F., Jendersie, S., Gourmelen, N., and Galton-Fenzi, B. K.: Subglacial Freshwater Drainage Increases Simulated Basal Melt of the Totten Ice Shelf, Geophysical Research Letters, 50, https://doi.org/10.1029/2023GL103765, 2023.

Hallberg, R.: Using a resolution function to regulate parameterizations of oceanic mesoscale eddy effects, Ocean Modelling, 72, 92–103, https://doi.org/10.1016/j.ocemod.2013.08.007, 2013.

Hattermann, T., Nst, O. A., Lilly, J. M., and Smedsrud, L. H.: Two years of oceanic observations below the Fimbul Ice Shelf, Antarctica, Geophysical Research Letters, 39, https://doi.org/10.1029/2012GL051012, 2012.

Hattermann, T., Smedsrud, L. H., Nøst, O. A., Lilly, J. M., and Galton-Fenzi, B. K.: Eddy-resolving simulations of the Fimbul Ice Shelf cavity circulation: Basal melting and exchange with open ocean, Ocean Modelling, 82, 28–44, https://doi.org/10.1016/j.ocemod.2014.07.004, 2014.

Hausmann, U., Sallée, J. B., Jourdain, N. C., Mathiot, P., Rousset, C., Madec, G., Deshayes, J., and Hattermann, T.: The Role of Tides in Ocean-Ice Shelf Interactions in the Southwestern Weddell Sea, Journal of Geophysical Research: Oceans, 125, https://doi.org/10.1029/2019JC015847, 2020.

Heuzé, C.: Antarctic Bottom Water and North Atlantic Deep Water in CMIP6 models, Ocean Science, 17, 59–90, https://doi.org/10.5194/os-17-59-2021, 2021.

Heywood, K. J., Schmidtko, S., Heuzé, C., Kaiser, J., Jickells, T. D., Queste, B. Y., Stevens, D. P., Wadley, M., Thompson, A. F., Fielding, S., Guihen, D., Creed, E., Ridley, J. K., and Smith, W.: Ocean processes at the Antarctic continental slope, Philosophical Transactions of the Royal Society A: Mathematical, Physical and Engineering Sciences, 372, https://doi.org/10.1098/rsta.2013.0047, 2014.

Holland, D. M. and Jenkins, A.: Modeling Thermodynamic Ice–Ocean Interactions at the Base of an Ice Shelf, Journal of Physical Oceanography, 29, 1787–1800, https://doi.org/10.1175/1520-0485(1999)029<1787:MTIOIA>2.0.CO;2, 1999.

Holland, P. R., Bracegirdle, T. J., Dutrieux, P., Jenkins, A., and Steig, E. J.: West Antarctic ice loss influenced by internal climate variability and anthropogenic forcing, Nature Geoscience, 12, 718–724, https://doi.org/10.1038/s41561-019-0420-9, 2019.

Jacobs, S., Giulivi, C., Dutrieux, P., Rignot, E., Nitsche, F., and Mouginot, J.: Getz Ice Shelf melting response to changes in ocean forcing, Journal of Geophysical Research: Oceans, 118, 4152–4168, https://doi.org/10.1002/jgrc.20298, 2013.

Jacobs, S. S., Helmer, H. H., Doake, C. S. M., Jenkins, A., and Frolich, R. M.: Melting of ice shelves and the mass balance of Antarctica, Journal of Glaciology, 38, https://www.cambridge.org/core., 1992.

Jacobs, S. S., Jenkins, A., Giulivi, C. F., and Dutrieux, P.: Stronger ocean circulation and increased melting under Pine Island Glacier ice shelf, Nature Geoscience, 4, 519–523, https://doi.org/10.1038/ngeo1188, 2011.

Jendersie, S., Williams, M. J., Langhorne, P. J., and Robertson, R.: The Density-Driven Winter Intensification of the Ross Sea Circulation, Journal of Geophysical Research: Oceans, 123, 7702–7724, https://doi.org/10.1029/2018JC013965, 2018.

https://doi.org/10.5194/egusphere-2024-3905
Preprint. Discussion started: 13 February 2025

Jenkins, A., Dutrieux, P., Jacobs, S. S., McPhail, S. D., Perrett, J. R., Webb, A. T., and White, D.: Observations beneath Pine Island Glacier in West-Antarctica and implications for its retreat, Nature Geoscience, 3, 468–472, https://doi.org/10.1038/ngeo890, 2010.

Joughin, I. and Padman, L.: Melting and freezing beneath Filchner-Ronne Ice Shelf, Antarctica, Geophysical Research Letters, 30, https://doi.org/10.1029/2003GL016941, 2003.

Joughin, I., Smith, B. E., Howat, I. M., Scambos, T., and Moon, T.: Greenland flow variability from ice-sheet-wide velocity mapping, Journal of Glaciology, 56, 415–430, https://doi.org/10.3189/002214310792447734, 2010.

Jourdain, N. C., Molines, J. M., Sommer, J. L., Mathiot, P., Chanut, J., de Lavergne, C., and Madec, G.: Simulating or prescribing the influence of tides on the Amundsen Sea ice shelves, Ocean Modelling, 133, 44–55, https://doi.org/10.1016/j.ocemod.2018.11.001, 2019.

Jourdain, N. C., Mathiot, P., Burgard, C., Caillet, J., and Kittel, C.: Ice Shelf Basal Melt Rates in the Amundsen Sea at the End of the 21st Century, Geophysical Research Letters, 49, https://doi.org/10.1029/2022GL100629, 2022.

Khazendar, A., Schodlok, M. P., Fenty, I., Ligtenberg, S. R., Rignot, E., and Broeke, M. R. V. D.: Observed thinning of Totten Glacier is linked to coastal polynya variability, Nature Communications, 4, https://doi.org/10.1038/ncomms3857, 2013.

Kim, T., Hong, J. S., Jin, E. K., Moon, J. H., Song, S. K., and Lee, W. S.: Spatiotemporal variability in ocean-driven basal melting of cold-water cavity ice shelf in Terra Nova Bay, East Antarctica: roles of tide and cavity geometry, Frontiers in Marine Science, 10, https://doi.org/10.3389/fmars.2023.1249562, 2023.

Kimura, S., Jenkins, A., Regan, H., Holland, P. R., Assmann, K. M., Whitt, D. B., Wessem, M. V., van de Berg, W. J., Reijmer, C. H., and Dutrieux, P.: Oceanographic Controls on the Variability of Ice-Shelf Basal Melting and Circulation of Glacial Meltwater in the Amundsen Sea Embayment, Antarctica, Journal of Geophysical Research: Oceans, 122, 10 131–10 155, https://doi.org/10.1002/2017JC012926, 2017.

Kusahara, K., Hasumi, H., and Tamura, T.: Modeling sea ice production and dense shelf water formation in coastal polynyas around East Antarctica, Journal of Geophysical Research: Oceans, 115, https://doi.org/10.1029/2010JC006133, 2010.

Kusahara, K., Tatebe, H., Hajima, T., Saito, F., and Kawamiya, M.: Antarctic Sea Ice Holds the Fate of Antarctic Ice-Shelf Basal Melting in a Warming Climate, Journal of Climate, 36, 713–743, https://doi.org/10.1175/JCLI-D-22-0079.1, 2023.

Kusahara, K., Hirano, D., Fujii, M., Fraser, A. D., Tamura, T., Mizobata, K., Williams, G. D., and Aoki, S.: Modeling seasonal-to-decadal ocean-cryosphere interactions along the Sabrina Coast, East Antarctica, Cryosphere, 18, 43–73, https://doi.org/10.5194/tc-18-43-2024, 2024.

Large, W. G., Mcwilliams, J. C., and Doney, S. C.: OCEANIC VERTICAL MIXING: A REVIEW AND A MODEL WITH A NONLOCAL BOUNDARY LAYER PARAMETERIZATION, 1994.

Lauber, J., Hattermann, T., de Steur, L., Darelius, E., Auger, M., Nøst, O. A., and Moholdt, G.: Warming beneath an East Antarctic ice shelf due to increased subpolar westerlies and reduced sea ice, Nature Geoscience, 16, 877–885, https://doi.org/10.1038/s41561-023-01273-5, 2023.

Lindbäck, K., Moholdt, G., Nicholls, K. W., Hattermann, T., Pratap, B., Thamban, M., and Matsuoka, K.: Spatial and temporal variations in basal melting at Nivlisen ice shelf, East Antarctica, derived from phase-sensitive radars, Cryosphere, 13, 2579–2595, https://doi.org/10.5194/tc-13-2579-2019, 2019.

Lindbäck, K., Darelius, E., Moholdt, G., Vankova, I., Hattermann, T., Lauber, J., and de Steur, L.: Basal melting and oceanic observations beneath Fimbulisen, East Antarctica, https://doi.org/10.22541/essoar.170365303.33631810/v1, 2023.

https://doi.org/10.5194/egusphere-2024-3905
Preprint. Discussion started: 13 February 2025

Liu, Y., Nikurashin, M., and Peña-Molino, B.: Seafloor roughness reduces melting of East Antarctic ice shelves, Communications Earth and Environment, 5, https://doi.org/10.1038/s43247-024-01480-x, 2024.

Makinson, K. and Nicholls, K. W.: Modeling tidal currents beneath Filchner-Ronne Ice Shelf and on the adjacent continental shelf: Their effect on mixing and transport, Journal of Geophysical Research: Oceans, 104, 13 449–13 465, https://doi.org/10.1029/1999jc900008, 1999.

Marsh, O. J., Fricker, H. A., Siegfried, M. R., Christianson, K., Nicholls, K. W., Corr, H. F., and Catania, G.: High basal melting forming a channel at the grounding line of Ross Ice Shelf, Antarctica, Geophysical Research Letters, 43, 250–255, https://doi.org/10.1002/2015GL066612, 2016.

Mazloff, M. R., Heimbach, P., and Wunsch, C.: An eddy-permitting Southern Ocean state estimate, Journal of Physical Oceanography, 40, 880–899, https://doi.org/10.1175/2009JPO4236.1, 2010.

Merino, N., Sommer, J. L., Durand, G., Jourdain, N. C., Madec, G., Mathiot, P., and Tournadre, J.: Antarctic icebergs melt over the Southern Ocean : Climatology and impact on sea ice, https://doi.org/10.1016/j.ocemod.2016.05.001, 2016.

Miles, B. W., Stokes, C. R., and Jamieson, S. S.: Pan-ice-sheet glacier terminus change in East Antarctica reveals sensitivity of Wilkes Land to sea-ice changes, Science Advances, 2, https://doi.org/10.1126/sciadv.1501350, 2016.

Milillo, P., Rignot, E., Rizzoli, P., Scheuchl, B., Mouginot, J., Bueso-Bello, J., and Prats-Iraola, P.: Heterogeneous retreat and ice melt of Thwaites Glacier, West Antarctica, Science Advances, 5, https://doi.org/10.1126/sciadv.aau3433, 2019.

Mosbeux, C., Padman, L., Klein, E., Bromirski, P. D., and Fricker, H. A.: Seasonal variability in Antarctic ice shelf velocities forced by sea surface height variations, Cryosphere, 17, 2585–2606, https://doi.org/10.5194/tc-17-2585-2023, 2023.

Nakayama, Y., Timmermann, R., Rodehacke, C. B., Schröder, M., and Hellmer, H. H.: Modeling the spreading of glacial meltwater from the Amundsen and Bellingshausen Seas, Geophysical Research Letters, 41, 7942–7949, https://doi.org/10.1002/2014GL061600, 2014.

Naughten, K. A., Meissner, K. J., Galton-Fenzi, B. K., England, M. H., Timmermann, R., Hellmer, H. H., Hattermann, T., and Debernard, J. B.: Intercomparison of Antarctic ice-shelf, ocean, and sea-ice interactions simulated by MetROMS-iceshelf and FESOM 1.4, Geoscientific Model Development, 11, 1257–1292, https://doi.org/10.5194/gmd-11-1257-2018, 2018.

Nicholls, K. W., Padman, L., Schröder, M., Woodgate, R. A., Jenkins, A., and Øterhus, S.: Water mass modification over the continental shelf north of Ronne Ice Shelf, Antarctica, Journal of Geophysical Research: Oceans, 108, https://doi.org/10.1029/2002jc001713, 2003.

Nicholls, K. W., Corr, H. F., Stewart, C. L., Lok, L. B., Brennan, P. V., and Vaughan, D. G.: Instruments and methods: A ground-based radar for measuring vertical strain rates and time-varying basal melt rates in ice sheets and shelves, Journal of Glaciology, 61, 1079–1087, https://doi.org/10.3189/2015JoG15J073, 2015.

Ohshima, K. I., Nihashi, S., and Iwamoto, K.: Global view of sea-ice production in polynyas and its linkage to dense/bottom water formation, https://doi.org/10.1186/s40562-016-0045-4, 2016.

Paolo, F. S., Fricker, H. A., and Padman, L.: Volume loss from Antarctic ice shelves is accelerating, Science, 348, 327–331, https://doi.org/10.1126/science.aaa0940, 2015.

Park, T., Nakayama, Y., and Nam, S. H.: Amundsen Sea circulation controls bottom upwelling and Antarctic Pine Island and Thwaites ice shelf melting, Nature Communications, 15, https://doi.org/10.1038/s41467-024-47084-z, 2024.

Pritchard, H. D., Ligtenberg, S. R., Fricker, H. A., Vaughan, D. G., Broeke, M. R. V. D., and Padman, L.: Antarctic ice-sheet loss driven by basal melting of ice shelves, Nature, 484, 502–505, https://doi.org/10.1038/nature10968, 2012.

Purich, A. and Doddridge, E. W.: Record low Antarctic sea ice coverage indicates a new sea ice state, Communications Earth and Environment, 4, https://doi.org/10.1038/s43247-023-00961-9, 2023.

https://doi.org/10.5194/egusphere-2024-3905
Preprint. Discussion started: 13 February 2025

Purich, A. and England, M. H.: Historical and Future Projected Warming of Antarctic Shelf Bottom Water in CMIP6 Models, Geophysical Research Letters, 48, https://doi.org/10.1029/2021GL092752, 2021.

Richter, O., Gwyther, D. E., Galton-Fenzi, B. K., and Naughten, K. A.: The Whole Antarctic Ocean Model (WAOM v1.0): Development and evaluation, Geoscientific Model Development, 15, 617–647, https://doi.org/10.5194/gmd-15-617-2022, 2022a.

Richter, O., Gwyther, D. E., King, M. A., and Galton-Fenzi, B. K.: The impact of tides on Antarctic ice shelf melting, Cryosphere, 16, 1409–1429, https://doi.org/10.5194/tc-16-1409-2022, 2022b.

Rignot, E., Jacobs, S., Mouginot, J., and Scheuchl, B.: Ice-Shelf Melting Around Antarctica, Science, 341, 266–270, https://doi.org/10.1126/science.1235798, 2013.

Rosevear, M. G., Gayen, B., Vreugdenhil, C. A., and Galton-Fenzi, B. K.: How Does the Ocean Melt Antarctic Ice Shelves?, Annual Review of Marine Science, 14, 37, https://doi.org/10.1146/annurev-marine-040323-074354, 2024.

Sallée, J.-B., Vignes, L., Minière, A., Steiger, N., Pauthenet, E., Lourenco, A., Speer, K., Lazarevich, P., and Nicholls, K. W.: Subsurface floats in the Filchner Trough provide the first direct under-ice tracks of the circulation on shelf, Ocean Science, 20, 1267–1280, https://doi.org/10.5194/os-20-1267-2024, 2024.

Schmidtko, S., Heywood, K. J., Thompson, A. F., and Aoki, S.: Multidecadal warming of Antarctic waters, Science, 346, 1227–1231, https://doi.org/10.1126/science.1256117, 2014.

Schnaase, F. and Timmermann, R.: Representation of shallow grounding zones in an ice shelf-ocean model with terrain-following coordinates, Ocean Modelling, 144, https://doi.org/10.1016/j.ocemod.2019.101487, 2019.

Seroussi, H., Verjans, V., Nowicki, S., Payne, A. J., Goelzer, H., Lipscomb, W. H., Abe-Ouchi, A., Agosta, C., Albrecht, T., Asay-Davis, X., Barthel, A., Calov, R., Cullather, R., Dumas, C., Galton-Fenzi, B. K., Gladstone, R., Golledge, N. R., Gregory, J. M., Greve, R., Hattermann, T., Hoffman, M. J., Humbert, A., Huybrechts, P., Jourdain, N. C., Kleiner, T., Larour, E., Leguy, G. R., Lowry, D. P., Little, C. M., Morlighem, M., Pattyn, F., Pelle, T., Price, S. F., Quiquet, A., Reese, R., Schlegel, N. J., Shepherd, A., Simon, E., Smith, R. S., Straneo, F., Sun, S., Trusel, L. D., Breedam, J. V., Katwyk, P. V., van de Wal, R. S., Winkelmann, R., Zhao, C., Zhang, T., and Zwinger, T.: Insights into the vulnerability of Antarctic glaciers from the ISMIP6 ice sheet model ensemble and associated uncertainty, Cryosphere, 17, 5197–5217, https://doi.org/10.5194/tc-17-5197-2023, 2023.

Seroussi, H., Pelle, T., Lipscomb, W. H., Abe-Ouchi, A., Albrecht, T., Alvarez-Solas, J., Asay-Davis, X., Barre, J. B., Berends, C. J., Bernales, J., Blasco, J., Caillet, J., Chandler, D. M., Coulon, V., Cullather, R., Dumas, C., Galton-Fenzi, B. K., Garbe, J., Gillet-Chaulet, F., Gladstone, R., Goelzer, H., Golledge, N., Greve, R., Gudmundsson, G. H., Han, H. K., Hillebrand, T. R., Hoffman, M. J., Huybrechts, P., Jourdain, N. C., Klose, A. K., Langebroek, P. M., Leguy, G. R., Lowry, D. P., Mathiot, P., Montoya, M., Morlighem, M., Nowicki, S., Pattyn, F., Payne, A. J., Quiquet, A., Reese, R., Robinson, A., Saraste, L., Simon, E. G., Sun, S., Twarog, J. P., Trusel, L. D., Urruty, B., Breedam, J. V., van de Wal, R. S., Wang, Y., Zhao, C., and Zwinger, T.: Evolution of the Antarctic Ice Sheet Over the Next Three Centuries From an ISMIP6 Model Ensemble, Earth's Future, 12, https://doi.org/10.1029/2024EF004561, 2024.

Shchepetkin, A. F. and McWilliams, J. C.: The regional oceanic modeling system (ROMS): A split-explicit, free-surface, topography-following-coordinate oceanic model, Ocean Modelling, 9, 347–404, https://doi.org/10.1016/j.ocemod.2004.08.002, 2005.

Silvano, A., Rintoul, S. R., and Herraiz-Borreguero, L.: Ocean-ice shelf interaction in East Antarctica, Oceanography, 29, 130–143, https://doi.org/10.5670/oceanog.2016.105, 2016.

Silvano, A., Rintoul, S. R., Peña-Molino, B., and Williams, G. D.: Distribution of water masses and meltwater on the continental shelf near the Totten and Moscow University ice shelves, Journal of Geophysical Research: Oceans, 122, 2050–2068, https://doi.org/10.1002/2016JC012115, 2017.

https://doi.org/10.5194/egusphere-2024-3905
Preprint. Discussion started: 13 February 2025

Silvano, A., Rintoul, S. R., Peña-Molino, B., Hobbs, W. R., van Wijk, E., Aoki, S., Tamura, T., and Williams, G. D.: Freshening by glacial meltwater enhances melting of ice shelves and reduces formation of Antarctic Bottom Water, Science Advances, 4, https://doi.org/10.1126/sciadv.aap9467, 2018.

Stammerjohn, S. E., Maksym, T., Massom, R. A., Lowry, K., Arrigo, K. R., Yuan, X., Raphael, M., Randall-Goodwin, E., Sherrell, R. M., and Yager, P. L.: Seasonal sea ice changes in the amundsen sea, Antarctica, over the period of 1979-2014, Elementa, 3, https://doi.org/10.12952/journal.elementa.000055, 2015.

Stern, A. A., Dinniman, M. S., Zagorodnov, V., Tyler, S. W., and Holland, D. M.: Intrusion of warm surface water beneath the McMurdo ice shelf, Antarctica, Journal of Geophysical Research: Oceans, 118, 7036–7048, https://doi.org/10.1002/2013JC008842, 2013.

Stewart, A. L., Klocker, A., and Menemenlis, D.: Circum-Antarctic Shoreward Heat Transport Derived From an Eddy- and Tide-Resolving Simulation, Geophysical Research Letters, 45, 834–845, https://doi.org/10.1002/2017GL075677, 2018.

Stewart, C. L., Christoffersen, P., Nicholls, K. W., Williams, M. J. M., and Dowdeswell, J. A.: Basal melting of Ross Ice Shelf from solar heat absorption in an ice-front polynya, Nature Geoscience, 12, 435–440, https://doi.org/10.1038/s41561-019-0356-0, 2019.

Sun, S., Hattermann, T., Pattyn, F., Nicholls, K. W., Drews, R., and Berger, S.: Topographic Shelf Waves Control Seasonal Melting Near Antarctic Ice Shelf Grounding Lines, Geophysical Research Letters, 46, 9824–9832, https://doi.org/10.1029/2019GL083881, 2019.

Tamura, T., Ohshima, K. I., and Nihashi, S.: Mapping of sea ice production for Antarctic coastal polynyas, Geophysical Research Letters, 35, https://doi.org/10.1029/2007GL032903, 2008.

Tamura, T., Ohshima, K. I., Nihashi, S., and Hasumi, H.: Estimation of surface heat/salt fluxes associated with sea ice growth/melt in the Southern Ocean, Scientific Online Letters on the Atmosphere, 7, 17–20, https://doi.org/10.2151/sola.2011-005, 2011.

Thompson, A. F., Stewart, A. L., Spence, P., and Heywood, K. J.: The Antarctic Slope Current in a Changing Climate, https://doi.org/10.1029/2018RG000624, 2018.

Timmermann, R. and Goeller, S.: Response to Filchner-Ronne Ice Shelf cavity warming in a coupled ocean-ice sheet model - Part 1: The ocean perspective, Ocean Science, 13, 765–776, https://doi.org/10.5194/os-13-765-2017, 2017.

Vaňková, I. and Nicholls, K. W.: Ocean Variability Beneath the Filchner-Ronne Ice Shelf Inferred From Basal Melt Rate Time Series, Journal of Geophysical Research: Oceans, 127, https://doi.org/10.1029/2022JC018879, 2022.

Vaňková, I., Cook, S., Winberry, J. P., Nicholls, K. W., and Galton-Fenzi, B. K.: Deriving Melt Rates at a Complex Ice Shelf Base Using In Situ Radar: Application to Totten Ice Shelf, Geophysical Research Letters, 48, https://doi.org/10.1029/2021GL092692, 2021.

Walker, D. P., Brandon, M. A., Jenkins, A., Allen, J. T., Dowdeswell, J. A., and Evans, J.: Oceanic heat transport onto the Amundsen Sea shelf through a submarine glacial trough, Geophysical Research Letters, 34, https://doi.org/10.1029/2006GL028154, 2007.

Walker, D. P., Jenkins, A., Assmann, K. M., Shoosmith, D. R., and Brandon, M. A.: Oceanographic observations at the shelf break of the Amundsen Sea, Antarctica, Journal of Geophysical Research: Oceans, 118, 2906–2918, https://doi.org/10.1002/jgrc.20212, 2013.

Webber, B. G., Heywood, K. J., Stevens, D. P., Dutrieux, P., Abrahamsen, E. P., Jenkins, A., Jacobs, S. S., Ha, H. K., Lee, S. H., and Kim, T. W.: Mechanisms driving variability in the ocean forcing of Pine Island Glacier, Nature Communications, 8, https://doi.org/10.1038/ncomms14507, 2017.

Wei, W., Blankenship, D. D., Greenbaum, J. S., Gourmelen, N., Dow, C. F., Richter, T. G., Greene, C. A., Young, D. A., Lee, S. H., Kim, T. W., Lee, W. S., and Assmann, K. M.: Getz Ice Shelf melt enhanced by freshwater discharge from beneath the West Antarctic Ice Sheet, Cryosphere, 14, 1399–1408, https://doi.org/10.5194/tc-14-1399-2020, 2020.

Yang, H., Kim, T. W., Kim, Y., Yoo, J., Park, J., and Cho, Y. K.: Variability of Inflowing Current Into the Dotson Ice Shelf and Its Cause in the Amundsen Sea, Geophysical Research Letters, 51, https://doi.org/10.1029/2023GL105404, 2024.

https://doi.org/10.5194/egusphere-2024-3905
Preprint. Discussion started: 13 February 2025

Yang, H. W., Kim, T. W., Dutrieux, P., Wåhlin, A. K., Jenkins, A., Ha, H. K., Kim, C. S., Cho, K. H., Park, T., Lee, S. H., and Cho, Y. K.: Seasonal variability of ocean circulation near the Dotson Ice Shelf, Antarctica, Nature Communications, 13, https://doi.org/10.1038/s41467-022-28751-5, 2022.